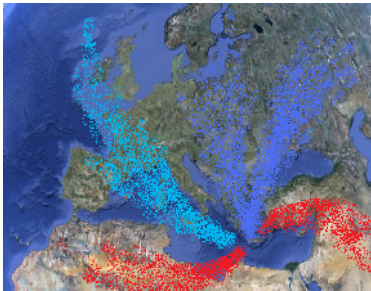
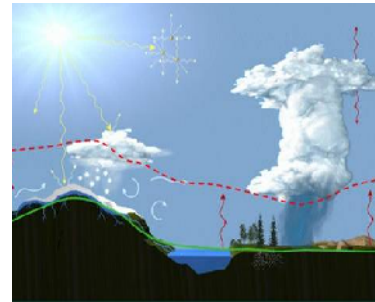
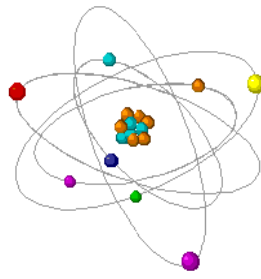


—

222



μ



$\mu/$

μ



:

,

2009

μ :

/ $\mu \mu$ μ ()

/ $\mu \mu$ μ

,

UNIVERSITY OF CRETE – DEPARTMENT OF CHEMISTRY

**MASTER OF SCIENCE – M.Sc.
ENVIRONMENTAL PROTECTION TECHNOLOGIES**

**STUDY OF THE TEMPORAL VARIATION OF RADON
222 IN THE MIXING LAYER AT FINOKALIA**

STRATAKI ANTHOULA

SUPERVISOR: KANAKIDOY MARIA

ENVIRONMENTAL CHEMICAL PROCESS LABORATORY
DEPARTMENT OF CHEMISTRY, UNIVERSITY OF CRETE

HERAKLIO 2009

$\mu \mu :$

μ	μ		
μ	μ	23	1980

	1998		
	1999-2004		$\mu \mu$
			,
			.
			: «
	2006		».
		μ	$\mu\mu$
	«		
		»	μ
	—		.

μ	μ		
	2004		/

	2004-2009		« . . . »
			. & . . »

	1997		(Lower)
--	------	--	---------

μ :

	iii
	vii
	1
Abstract	2
1.	3
2.	6
2.1.	6
2.1.1.	6
2.1.2.	μ	7
2.1.3.	9
2.1.4.	10
2.2.	μ μ	12
2.3.	μ	13
2.4.	13
2.5.	μ	16
2.6.	19
2.6.1.	μ μ	19
2.6.1.1.	μ μ	20
2.6.1.2.	μ μ	23
2.6.1.3.	μ	24
2.6.1.4.	μ	25
2.6.2.	μ μ ^(222Rn)	26
2.6.3.	μ μ	27
2.6.4.	28
3.	μ μ -	32
μ	32
3.1.	32
3.2.	:	32
3.3.	μ	33
3.4.	μ μ	35
3.5.	μ	40
3.6.	μ μ μ	2002-
2006.	42
4.	μ μ	47
4.1.	μ	47
4.2.	μ μ	57
μ	57
4.3.	μ μ μ	60
4.3.1.	μ μ	60
4.3.2.	μ 2004-2006.....	61
4.4.	μ μ	64
4.4.1.	μ	66
4.4.2.	μ	67
4.4.3.	μ	68

4.4.4.	μ	69				
4.4.5.	μ	70				
4.4.6.		70				
4.5.	μ	71				
4.6.	μ	μ	μ	76			
4.6.1.		(Urbino).	76			
4.6.2.	(,).....	77			
4.6.4.	Hok Tsui, Gosan	Mauna Loa.	79			
4.7.		81				
5.	$\mu\mu$	μ	μ	μ	82	
SPSS.							
5.1.	$\mu\mu$	μ	(Simple Linear Regression).		82	
5.2.	$\mu\mu$	μ	(Multiple Linear Regression).		84	
5.3.	$\mu\mu$	μ	μ	μ	,	,	
μ	μ	μ	μ	μ	μ	85
5.4.	$\mu\mu$	μ	μ	μ	μ	μ	
,	,	μ	μ	μ	μ	87
6.	μ	μ	μ	μ	μ	89	
6.1.	μ	μ			89	
6.2.					89	
6.2.1.					90	
6.2.2.		μ			92	
6.3.	μ	μ			93	
6.5.					98	
7.	μ	μ	μ	μ	μ	107	
7.1.	μ	μ			107	
7.2.					110	
					111	
μ	:				115	
μ	:	μ			117	
μ	III:				118	

1.	$\mu\mu$	6
2.	μ	10
3.	-238.	11
4.	-235.	12
5.	μ μ	13
6.	μ	14
7.	μ μ μ μ	17
8.	μ μ	18
9.	μ	21
10.	μ μ μ	21
11.	μ μ μ	22
12.	μ	25
13.	μ μ	26
14.	μ μ	26
15.	$\mu\mu$ μ	29
16.	μ 218 μ μ () DNA	30
17.		30
18.		31
19.	μ	32
20.	Thermo electron model 49C, μ	33
21.	μ μ	34
22.	$\mu\mu$ μ) (pCi/m ³),) (%)) (ppbv),) μ (C) μ (m/s),) (Watt/m ²) 2001-2006.	36
23.	μ	40
2002.		40
24.	μ	40
2003.		41
25.	μ	41
2004.		41
26.	μ	41
2005.		41
27.	μ 2006	41
28.	μ μ μ 2002-2006	43
pCi/m ³ .		45
29.	μ 2002 – 2006.	45
30.	μ μ μ	45
μ		46
31.	μ μ μ 2002-2006.	46

32.	μ μ μ	μ μ	2002-2006.....	46
33.	μ μ	μ	2002-2006.....	46
34.)	μ ,		
) μ	, μ)		
22/10/2005.....				48
35.)	μ ,		
) μ	,	μ		
26/03/2005.....				49
36.	μ μ μ	μ μ	0:00 26/03/2005 μ μ	
μ 12:00.....				49
37.)	μ ,		
) μ	,	μ 22		
23/02/2005.....				51
38.)	- μ		
) μ	,	28/01/2005.....		52
39.)	- μ)		
μ	,	20/08/2005.....		52
40.)	μ ,		
) μ	,			
μ 03/08/2005-04/08/2005.....				53
41.)	μ ,)		
μ	,)		
04/02/2005 08/02/2005.....				54
42.)	μ)		
μ)			
μ μ	01/04/2005-06/04/2005.....			56
43.	μ μ μ	μ μ	2002-	
2006 μ μ μ μ			57
44.	μ	μ μ μ		
.....				58
45.	μ	μ		58
46.	μ μ	μ μ)) μ	
.....				59
47.	μ μ	μ μ)) μ	
.....				60
48.	μ	-μ	2004.....	61
49.	μ	-μ	2005.....	61
50.	μ	- μ	2006.....	62
51.	μ	- μ	2002-2006.....	62
52.	μ μ	μ μ	μ (μ) (, ,)	
μ (, ,)	2004-2006.....			63
53.		μ μ		
.....				64
54.	μ μ	μ μ		
2002-2006. (, , , ,).....				65

55.	μ	μ	μ	μ	2002-2006	
(, , , ,)						65
56.	μ	25/01/2005	29/01/2005	, 10	μ	67
57.						68
58.					10	04/02/2005
08/02/2005						69
59.			μ			69
60.	μ	04/08/2003-11/08/2003				70
61.			μ	2006	μ	(1961-1990) 71
62.			μ	2006	μ	(1961-1990) 72
63.	μ					2006 72
64.	μ	1961-1990		2006		73
65.			μ	2006	μ	(1961-1990) 73
66.			μ	5	2006	74
67.	2003-2006	μ	(1961-1990)			75
68.	2 μ	μ	μ	μ	μ	²²² Rn
				²²² Rn	μ	μ
69.	μ	μ		μ		76
70.	μ	μ		μ		77
71.			μ	μ	μ	μ
			(,	VA)	77
72.			μ		,	μ
						78
73.			μ		,	μ
						78
74.			Alligator Rivers			78
75.	μ	μ			Nabarlek	1998 1999 79
76.	μ	μ			Djarr Djarr	1998 1999 79
77.	μ) Hok Tsui,) Gosan) Mauna Loa 80
78.	(a-c)		μ		(d-f)	Hok Tsui, Gosan Mauna Loa 2001 81
79.				μ		2002-2006 81

80.				μ		2002-2006.	
						81
81.	μ	μ		$\mu\mu$		μ	μ
	μ					μ	μ
82.		μ		μ		μ	
						95
83.		μ		μ		μ	
						95
84.		μ		S_4^{2-}		μ95
85.		μ		$C_2O_4^{2-}$		μ96
86.		μ		NH_4^+		μ96
87.		μ		$C_2O_4^{2-}$		μ96
88.		μ		NH_4^+		μ96
89.						μ	
	μ	1:5		$\mu\mu$		115
90.	μ	μ				116
91.			μ		μ	μ117
92.	μ					118
93.	μ					119
94.	$\mu\mu$	Feynman.				119
95.	μ	$\mu\mu$				120

1.	μ	-	^{222}Rn	7				
2.			μ	8				
3.	μ			9				
4.			μ	13				
5.	μ	μ		15				
6.			μ	16				
7.			μ	Pasquill.....	24				
8.		μ	μ	26				
9.	μ	μ		28				
10.			μ	29				
11.			μ	29				
12.		μ	μ	μ	μ	μ	34	
13.			μ	μ	μ	35		
14.	$\mu\mu$		μ	μ	μ	μ	μ	37
15.			μ	2002-2006.....	37				
16.	μ	pCi/m^3		2002 μ	37			
17.	μ	pCi/m^3		2003 μ	38			
18.	μ	pCi/m^3		2004 μ	38			
19.	μ	pCi/m^3		2005 μ	38			
20.	μ	μ	μ	μ	μ	pCi/m^3	2006 μ	39
21.	μ			2002-2006.....	42				
22.		μ	μ	2004-2006.....	61				
23.	μ			μ	μ	-	62	
24.			μ	μ	^{222}Rn	76		
25.	μ	μ	μ	μ	μ	μ	85	
26.	$\mu\mu$		μ	μ	88			

27.		μ	88
μμ		μ	
28.		μ	93
29.		μ	94
30.		μ	μ
31.		Kaiser-Meyer-Olkin	97
μ		Kaiser-Meyer-Olkin	98
32.		Kaiser-Meyer-Olkin	98
μ		Kaiser-Meyer-Olkin	98
33.		Kaiser-Meyer-Olkin	98
10.		Kaiser-Meyer-Olkin	98
34.		μ	μ100
35.		μ	μ100
36.		μ	μ101
10,(). μ Varimax	102
μ		μ Varimax	103
μ		μ Varimax	104
10		μ Varimax	104

(²²²Rn). 226

2002 2006

2002-2006

23,31 pCi/m³
9,80 pCi/m³

137,40 pCi/m³

56,57 pCi/m³ ±

(emanation),

SPSS

NO₃⁻, NH₄⁺

(SO₄²⁻, C₂O₄²⁻,

Abstract.

The main purpose of this study was to investigate the variability of the atmospheric radon (^{222}Rn) concentration. Radon is a radioactive element produced during the radioactive decay series of radium (^{226}Ra) by ejecting an alpha- particle. In the present work we investigate the reasons for the gradient change in the concentration of radon and the mechanisms that control this change on Crete. For achieving this, targeted five year data (2002-2006) were used, from year 2002 to year 2006, from the monitoring station of Finokalia in the area of Lasithiou Crete. Using these data, meteorological parameters (wind speed and direction, relative humidity, temperature) and ozone, conclusions are drawn for the daily, annually and seasonally variability of radon.

The period 2002-2006 is characterized by daily average concentration of radon of $56,57 \text{ pCi/m}^3 \pm 23,31 \text{ pCi/m}^3$ and minimum maximum concentrations $9,805 \text{ pCi/m}^3$, $137,40 \text{ pCi/m}^3$, respectively. The concentration of radon is related mainly with a) the accumulation of radon, during days that wind speed is very low and the conditions of the atmospheric boundary layer are stable, b) the air mass movement and transfer of air masses rich in radon that have passed over land a few days before the observation. c) the conditions that dominate in the atmospheric boundary layer, since days that are characterized by intense temperature inversion during the night favour the accumulation of radon.

In the present study radon was correlated not only with meteorological parameters and ozone but also with fine and coarse aerosols. The correlations were made by the mean of the statistical programme SPSS and the analytical methods simple and multiple linear regression and principle components analysis.

The main conclusions drawn are summarized as follows: summer and fall are the seasons during which the transport of air masses affects most the concentration of radon. The wind speed modulates the concentration of radon because it affects its accumulation and long range transport. Synoptic scale meteorological phenomena can impress the movement and the stability of the atmospheric boundary layer and ultimately the concentration of radon. Radon was proved to be a good tracer for the evolution of the atmospheric boundary layer.

The correlation of radon with the fine and coarse fraction of aerosols indicate that the seasonality of radon is closer to the seasonality of the fine particles. Principle components analysis shows that radon can coexist with secondary particles, from anthropogenic activity (SO_4^{2-} , $\text{C}_2\text{O}_4^{2-}$, NO_3^- , NH_4^+) whereas it doesn't show any correlation with the ions and elements from the earth's crust.

iii) μ

μ

iv) μ

μ

μ

10^{-}

μ

μ

μ

.

μ

μ

,
,

μ

μ

$\mu\mu$

,

μ

μ

μ

.

μ

.

μ

.

μ

μ

μ

$\mu\mu$

μ

μ

μ

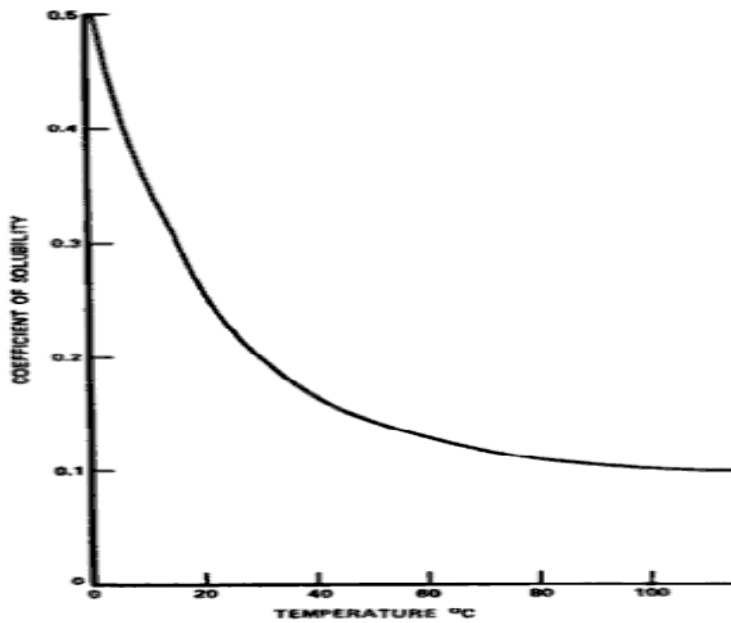
.

2. .

2.1. .

2.1.1. .

μ , μ μ ,
 μ , μ , μ , μ
 μ μ , μ . μ , μ 1.
 μ , μ . . .
 μ clathrate-hydrate μ , Rn-6H₂O
 (Martinelli, 1993). μ



1. $\mu\mu$

C_w/C_a , C_w C_a μ
 . (C. Richard Cothorn, 1987)

	μ
μ , μ , μ μ μ μ μ μ μ	μ , Rn, 86 μ 222g mol^{-1} $[e] 4f^{14}5d^{10}6s^26p^6$ $-61,8^\circ\text{C}$ 2, 8, 18, 32, 18, 8
	μ
μ μ μ μ (μ) μ , μ : 0°C 20°C 37°C 100°C μ 18 $^\circ\text{C}$: ()	-71°C 104°C 62 atm $9,96\text{kg/m}^3$ 0,507 0,250 0,167 0,106 16,56 29,00 9,20 13,24

1. μ – ^{222}Rn (National Council on Radiation Protection and Measurements, NCRP).

2.1.2. μ .

μ 1900
16 Agricola George (George Bauer:
, μ) 1957
 μ μ Schneeberg,
Erzgebirge (Ore mountains) (Lutz W. Weber, 2002).
 μ
Jachymov. μ μ μ μ
 μ μ :
 μ μ .
IUPAC (International Union and Pure and Applied Chemistry)
(Partington, J.R. 1957; Geiger and Szeel, 1900)
1900 μ μ
Friedrich Ernest Dorn. 1900 Friedrich Ernest Dorn μ
.. (Radium Emanation). μ Friedrich Ernest Dorn μ
 μ μ

Ernest Rutherford, Frederick Soddy, Marie and Pierre Curie,
 William Crookes, Andre Debierne, J.J. Thomson.
 Henri Becquerel, 1896

1597	agricola Erz.
1896	Becquerel
1898	Curie Schmidt
1898	Rutherford
1899	Thomson Rutherford
1899	Rutherford (emanation) « μ »
1900	Dorn ^{238}U (emanation)
1901	Rutherford Brooks
1901	Curie Rutherford
1902	Rutherford Soddy
1902	Thomson
1903	Rutherford Soddy
1904	Geisel Debierne

2.
 1898, Pierre Marie Curie
 Marie Curie
 1899, Pierre Marie Curie
 Robert B. Owens Ernest Rutherford
 Rutherford
 «Thorium Emanation». 1901 Marie Curie Dorn
 1903,

Andre – Louis Debierne (Actinium Emanation Ac Em). μ

2.1.3.

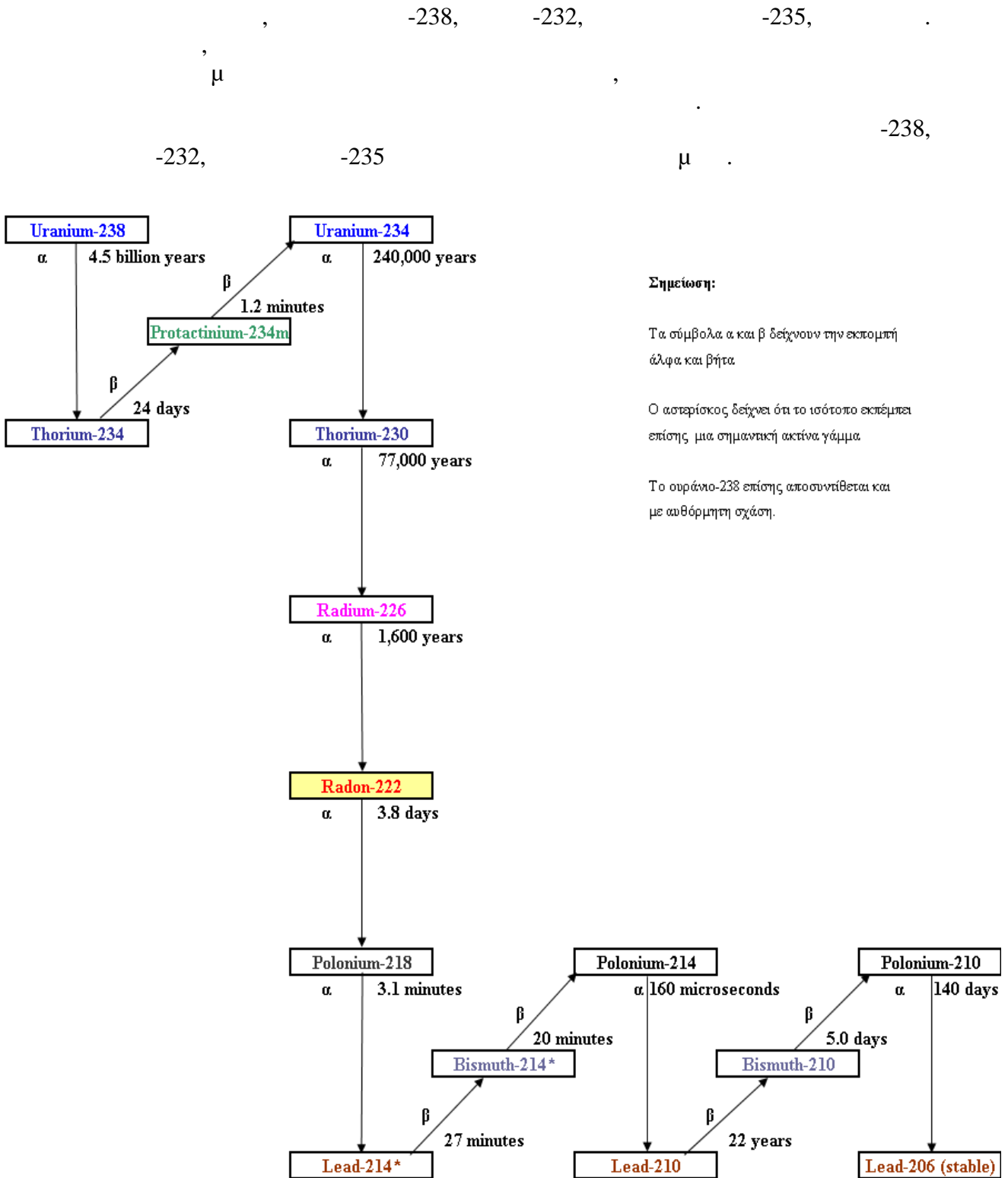
27 ^{200}Rn ^{226}Rn .
 μ μ 219, 220 222.
 (p)
 μ μ μ μ μ μ μ μ
 , μ ^{220}Rn ^{222}Rn μ μ μ μ
 0,72% ^{235}U , μ
 μ μ μ μ ^{235}U μ μ ^{219}Rn μ
 (HEU), μ
 To ^{222}Rn μ μ 3,8 μ , μ ^{220}Rn μ
 μ μ μ μ μ μ
 ^{219}Rn . μ μ
 ^{222}Rn , ^{220}Rn ^{220}Rn

		μ
^{219}Rn :		3,96 seconds
^{220}Rn :		56 seconds
^{222}Rn :	-232 - 226.	3,8 days
	-238.	

3. μ

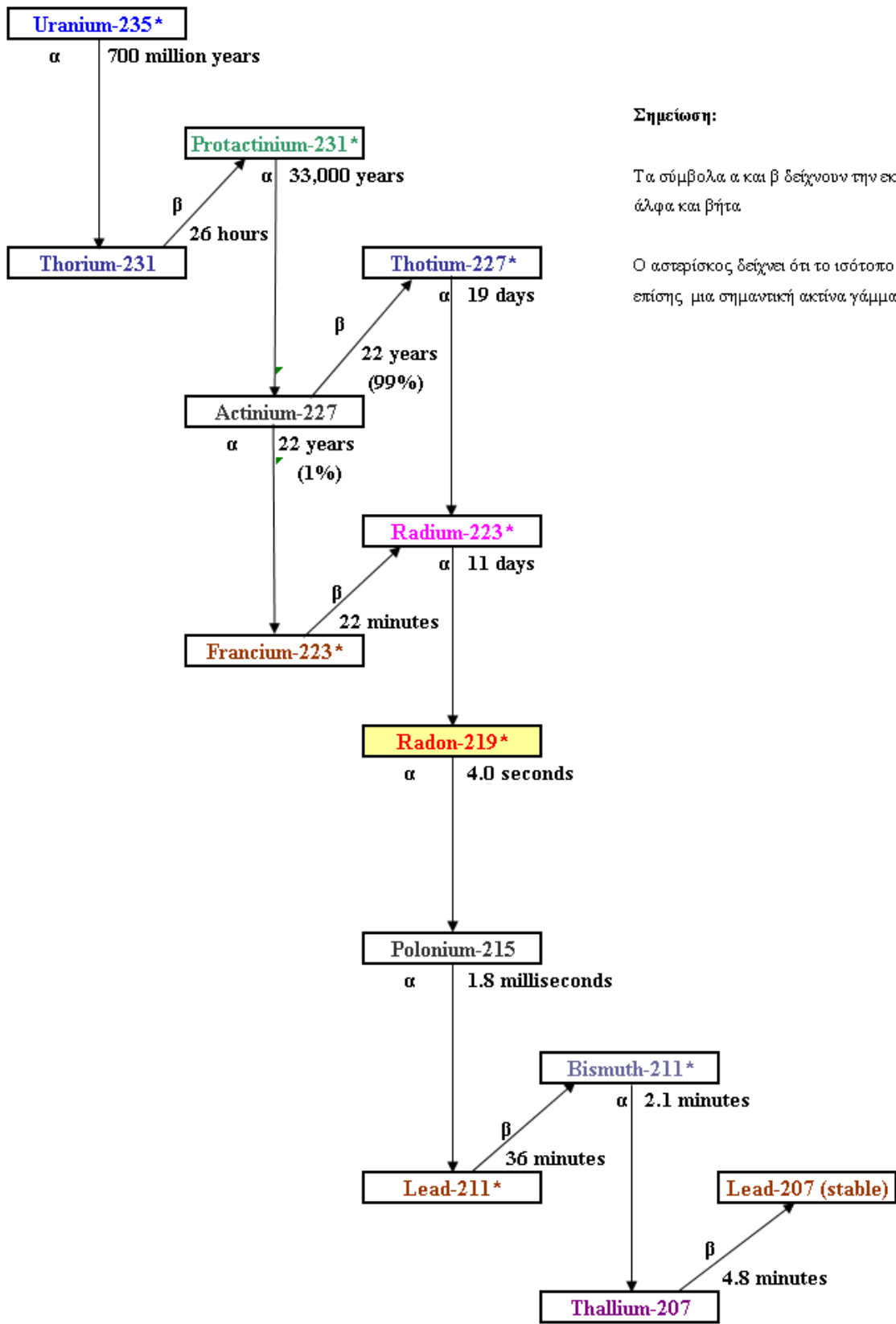
μ
2 4.

2.1.4.



2. Cothern, 1987; W. R. Van Schmus, 1995).

-238 (C. Richard



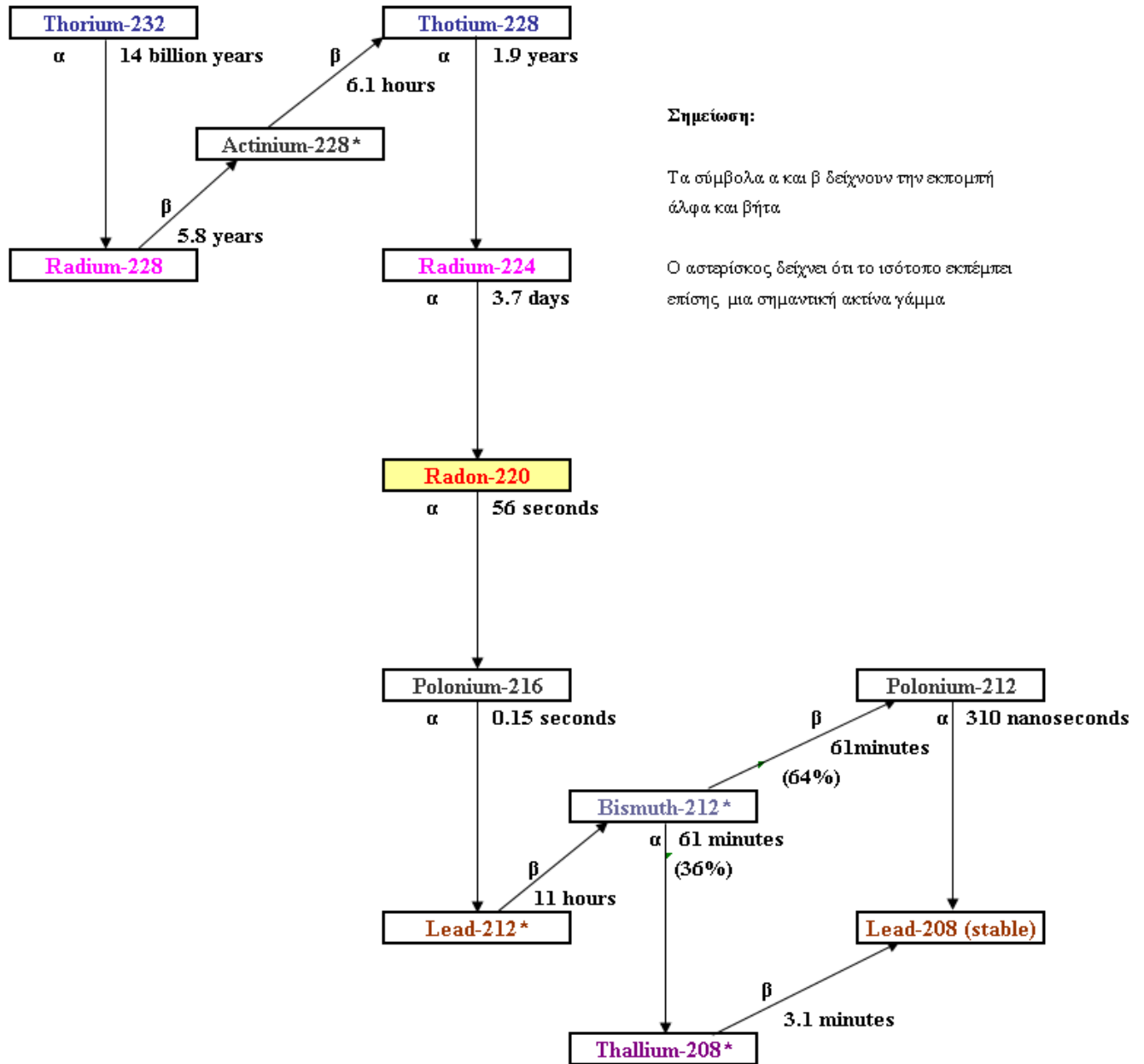
Σημείωση:

Τα σύμβολα α και β δείχνουν την εκπομπή άλφα και βήτα

Ο ασταρικός δείχνει ότι το ισότοπο εκπέμπει επίσης μια σημαντική ακτίνα γάμμα

3. Cothern, 1987; W. R. Van Schmus, 1995).

-235 (C. Richard



Σημείωση:

Τα σύμβολα α και β δείχνουν την εκπομπή άλφα και βήτα

Ο ασταρικός δείχνει ότι το ισότοπο εκπέμπει επίσης μια σημαντική ακτίνα γάμμα

4.

-232 (C. Richard

Cothorn, 1987; W. R. Van Schmus, 1995).

μ μ , μ . μ

II.

2.2. μ μ .

μ μ , 3,8 μ . μ -222, -

226 -238. μ μ

μ μ , , .
 :
 μ , , Radium Hill
 :
 μ (Sierra Albarrana, μ , μ (μ),
 , μ).
 :
 μ (Bergen -
 Vogtland) μ
 (Minas Gerais) .
 μ μ ,
 μ

Rock Type	Th (ppm)	U (ppm)	K (%)	Th/U	K/U	Th/K
Igneous						
Ultrabasic	0.02	0.007	0.01	2.8	1.4	2.0
Basic	3.4	0.8	1.0	4.3	1.3	3.4
Basic- intermediate	6.1	1.7	1.9	3.6	1.1	3.2
Intermediate	9.8	3.0	2.4	3.3	0.8	4.1
Intermediate-Acidic	16.0	3.6	3.0	4.4	0.8	5.3
Acidic	21.9	4.1	3.5	5.3	0.9	6.3
Sedimentary						
Evaporite	0.4	0.1	0.1	4.0	1.0	4.0
Carbonate	1.6	1.6	0.3	1.0	0.2	5.9
Sandstone	5.7	1.9	1.2	3.0	0.6	4.8
Shale	11.2	3.7	2.7	3.1	0.7	4.1
Metamorphic						
Amphibolite	2.0	0.9	0.6	2.2	0.7	3.3
Greenstone	3.4	0.8	1.0	4.3	1.3	3.4
Graywacke	6.7	2.1	2.8	3.2	1.3	2.4
Gneiss	10.6	2.3	3.4	4.6	1.5	3.1
Schist	13.5	4.1	2.5	3.3	0.6	5.5

5. μ μ ,
 μ (W. R. Van Schmus, 1995).

Rock Type	High	Moderate	Low
Igneous			
Granite	X		
Syenite	X		
Pegmatite	X		
Rhyolite	X		
Diorite		X	
Gabbro			X
Basalt			X
Diabase			X
Ultramafic			X
Metamorphic			
Gneiss (general)	←————→		
Schist (general)	←————→		
Marble			X
Slate			X
Quartzite			X
Sedimentary			
Sandstone	←————→		
Shale	←————→		
Carbonate (pure)			X
Siltstone	←————→		

6. μ (Stanley S. Johnson, 1991).

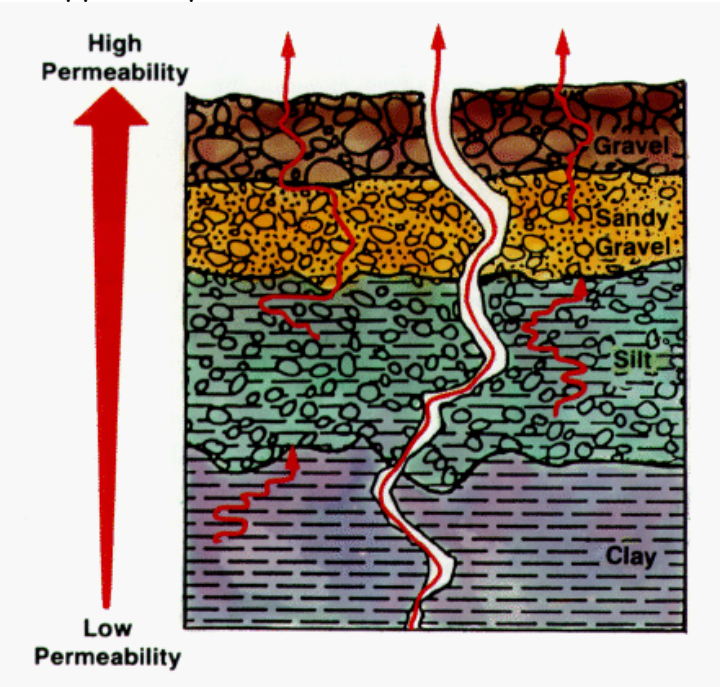
2.5. μ .

μ μ μ .

μ μ μ :

- μ μ μ
- μ μ μ
- μ μ μ

μ .



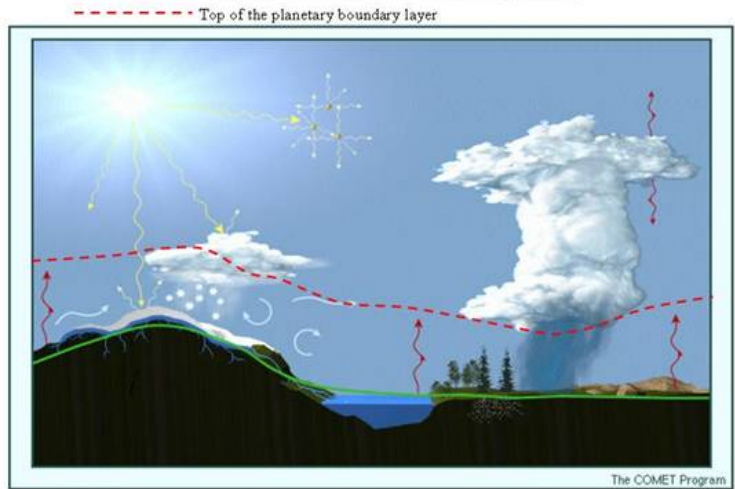
8.

<http://www.energy.cr.usgs.gov/radon/georadon/page10.gif>.

(Tanner 1980; Thamer et al. 1981).

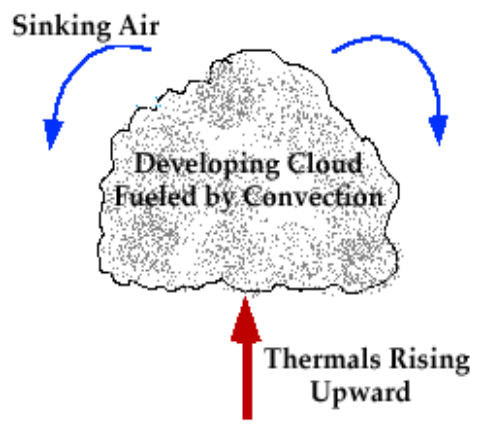
(Washington and Rose 1990),

Depiction of various surfaces and PBL processes



9. μ (:<http://www.esrl.noaa.gov/research/pbl>).

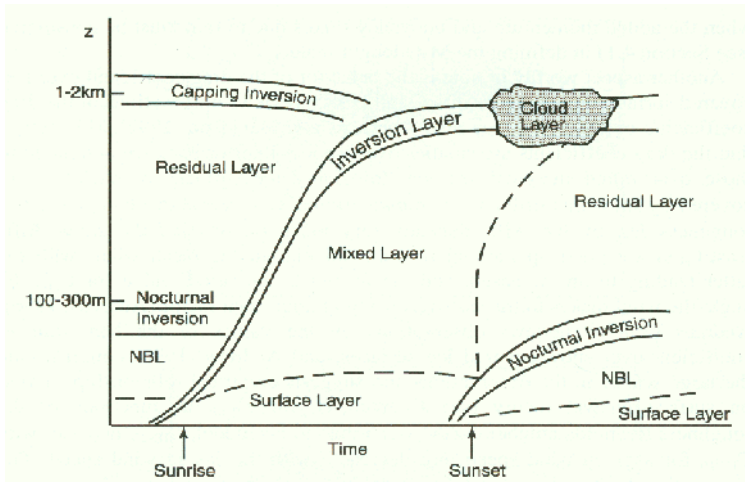
μ (h) μ (Gryning et al., 1987).
 μ (Convective boundary layer CBL), μ
 μ (CBL), μ
 μ , μ
 μ , μ
 μ , μ



10. μ (:[http://ww2010.atmos.uiuc.edu/\(Gh\)/wwhlpr/convection.rxml](http://ww2010.atmos.uiuc.edu/(Gh)/wwhlpr/convection.rxml)).

μ (Thermals). μ μ
 μ μ

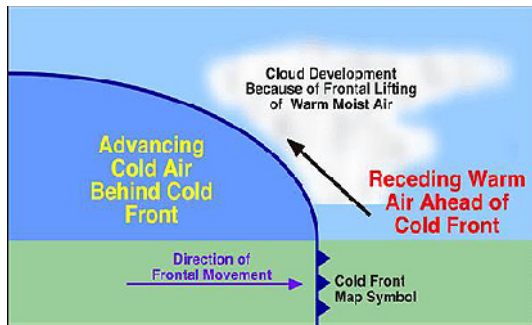
CBL.



11. (: Wyngaard, 1992)

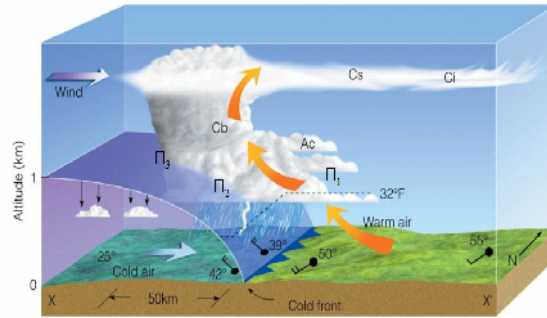
1.
 - 5-10% CBL.
2. (Mixed Layer)
 - (thermals)
 - updrafts (), (free convection).
 - downdrafts (), (forced convection).

3. (entrainment zone)



13.

(http://www.fas.org/irp/imint/docs/rst/Sect14/Sect14_1c.html).



14.

(<http://www.grossmont.edu/scotttherkalsen/physical/lectureresources/lectures.htm>).

	(1)	(2)	(3)
	-	, -	-
	Ci, Cs, Cu, Cb	Cu, Cb	Cu

8.

1, 2, 3, 14, (: « » , 2008).

2.6.2.

(²²²Rn) (CTMs) (GCMs) ²²²Rn.

^{222}Rn (Genthon and Armengaud (1995))
 GCMs.
 i. (Subgrid mixing schemes) (Brost and Chatfield, 1989; Jacob and Prather, 1990; Fiechter and Crutzen, 1990; Rind and Lerner, 1996; Allen et al, 1996)
 ii. (Petersen et al, 1998).
 iii. (Jacob et al, 1997; Raschet al, 2000)
 iv. (Manowald et al, 1997; Olive et al, 2004).

2.6.3.

(Connor et al., 1996, Segovia et al., 1997, 1999, 2003, Monnin and Seidel, 1997, Watananikorn, et al., 1998; Walia et al., 2003; Planinie et al., 2004, Yasuoka et. al., 2005, Imme et al., 2006, C. Papastefanou et al., 2001).
 CO_2 . Tashkent ()
 1966 (Ulamov and Mavasher, 1967).

2.6.4.

	μSv (mSv)
μ	0,4 0,5
()	1,2
(,)	0,3
	2,4

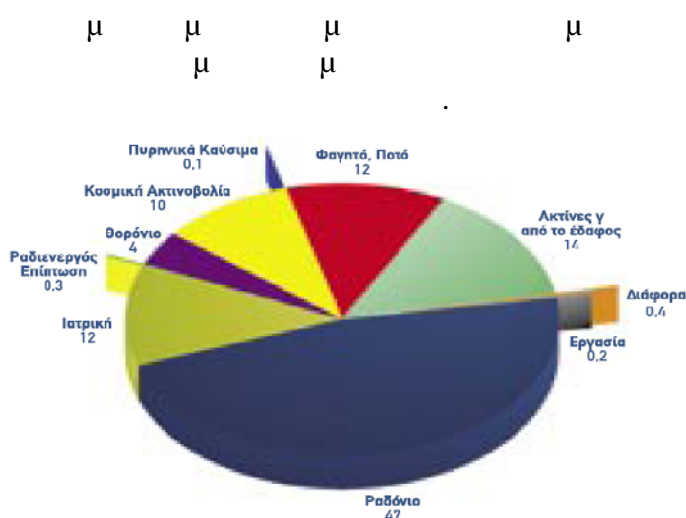
9. (: United Nations Scientific Committee on the effects of Atomic Radiation 2000).

	μ	μ 1.000	μ (mSv)
IV	<1.000	920	1,2
	1.000-3.000	150	0,14
	3.000-10.000	20	0,02
	>10.000	<20	<0,02
	μ μ	330	0,4

10. (: United Nations Scientific Committee on the effects of Atomic Radiation 2000).

μ / μ	μ (μ)	(mSv)
μ (μ μ)	800	1,8
μ	700	0,5
μ	420	0,2
/	2320	0,3
.	360	0,1
	4600	0,6
μ (μ)	250	3,0
(μ)	760	2,7
μ μ	3910	0,7
μ	300	1,0
μ	1250	4,8
μ	6500	1,8

11. (: United Nations Scientific Committee on the effects of Atomic Radiation 2000).



15. (: United Nations Scientific Committee on the effects of Atomic Radiation 2000).

^{238}U ^{232}Th ^{222}Rn ^{220}Rn ^{218}Po ^{214}Pb , ^{214}Bi , ^{214}Po

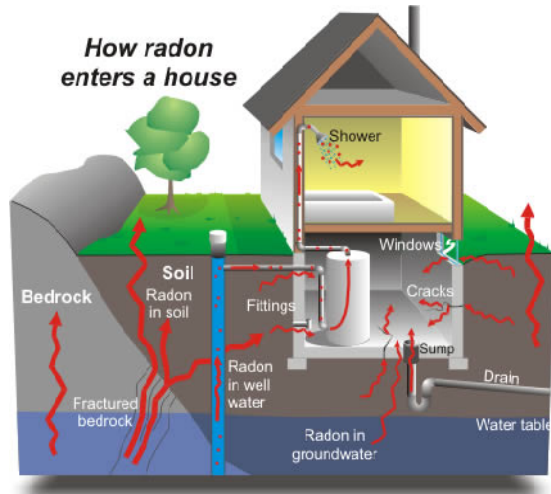
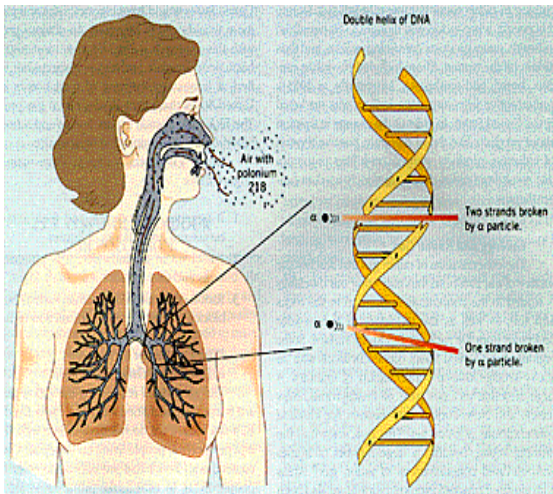
(, 16).

(,) ^{218}Po

(LET: linear

DNA

energy transfer)



16. 218

DNA (: http://enhs.umn.edu/hazards/hazardssite/radon/radon_molaction.html).

17. (: http://www.radon-services.com/diagrams/how_radon_enters.htm).

, 50%

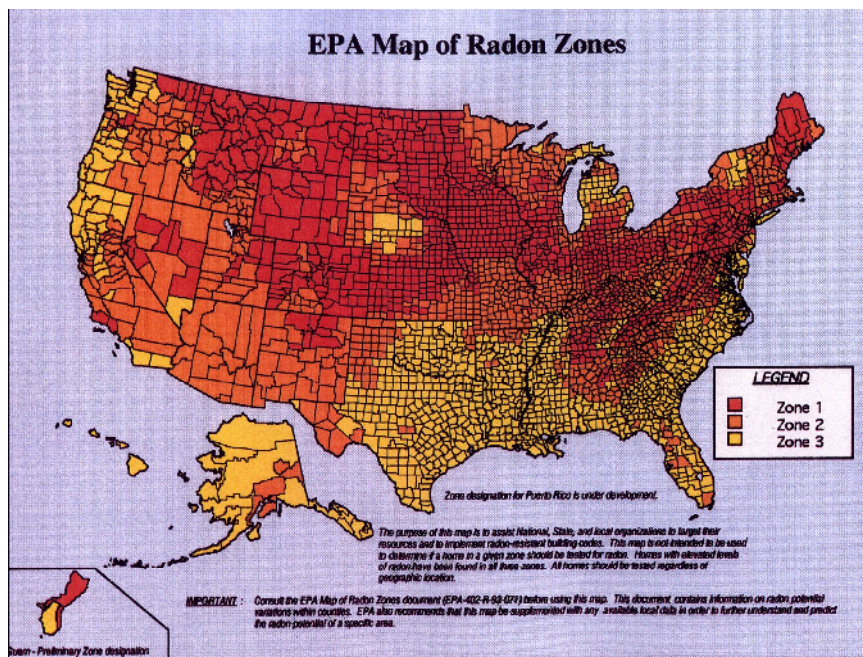
,

:

,

(AS) : «

15.000
 10
 (WHO
 IARC
 1988
 1988
 1988

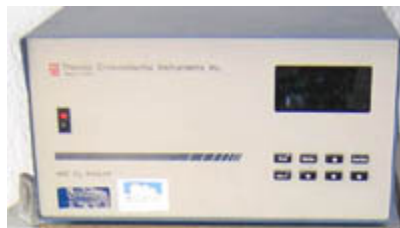


18. (: http://www.nationalsafety.biz/radon/EPA_Map_of_Radon_Zones.htm).

μ 5 min μ μ
 ppb_v. 254 nm.
 μ μ UV
 μ , μ μ Beer-Lambert:

$$\frac{I}{I_0} = e^{-KLC} \quad (E .1)$$

:	: μ	308cm ⁻¹ , 0 C, 1atm
	L: μ	
	C: ppm,	
	I: μ μ	(sample gas)
	I ₀ :	(reference gas)



20. Thermo electron model 49C, μ
 (<http://finokalia.chemistry.uoc.gr/>).

μ *PM*₁₀.

μ 10 μ Eberline FH 62I-R (Eberline Instruments
 GmbH), μ
 μ μ μ
 (-attenuation) (Gerasopoulos et al., 2006).

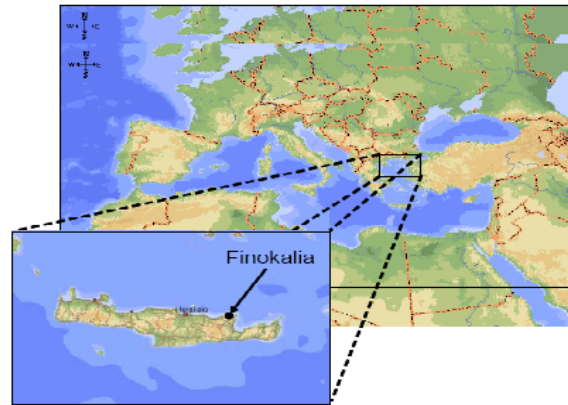
μ .

μ μ μ
 μ (IC) μ
 (Cl⁻, Br⁻, NO₃⁻, SO₄²⁻, C₂O₄²⁻, MS⁻) (Na⁺, Mg²⁺,
 Ca²⁺). (Ti, V, Cr, Mn, Fe, Ni, Cu, Zn, Cd, Pb)
 μ μ μ μ μ μ (ICP-
 MS). (OC
 EC) μ - μ μ μ (thermal-optical transmission
 method), μ μ μ Sunset
 Laboratory Inc. Oregon (E. Koulouri et al., 2008).

3.3. μ .

μ μ μ , μ .
 μ μ μ , μ μ .

5, .
 (five day back trajectories)
 HYSPLIT NOAA (HYbrid Single Particle Lagrangian Integrated Trajectory).

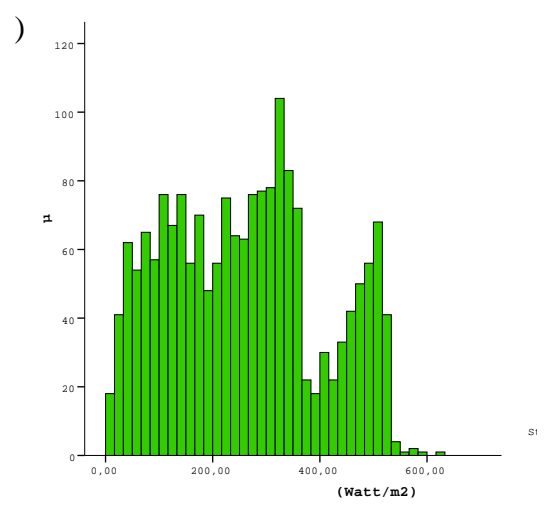
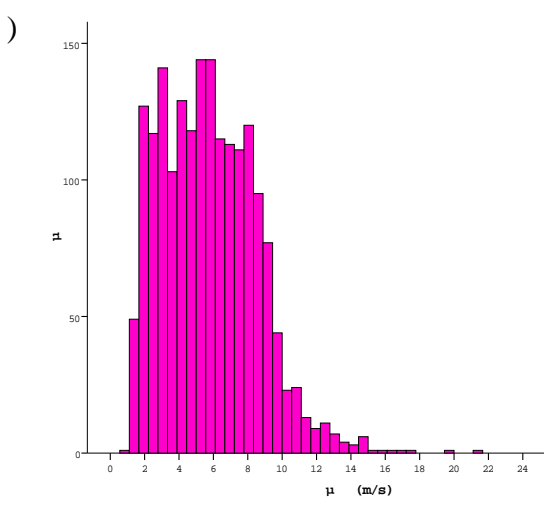
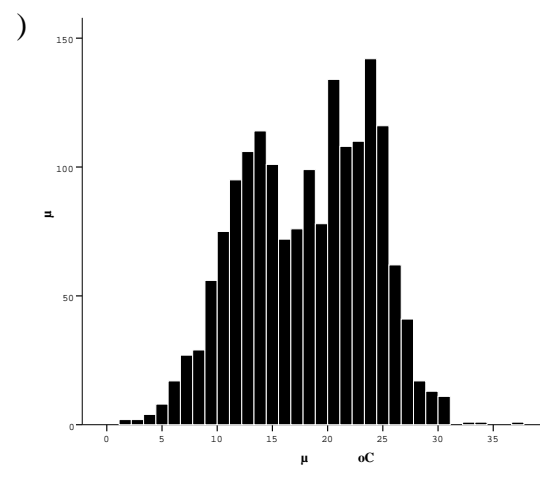
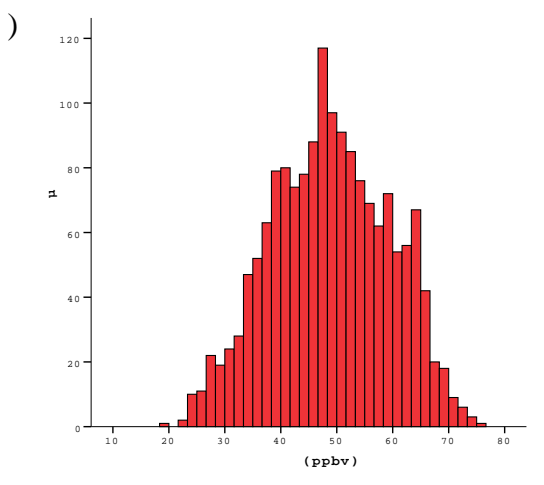
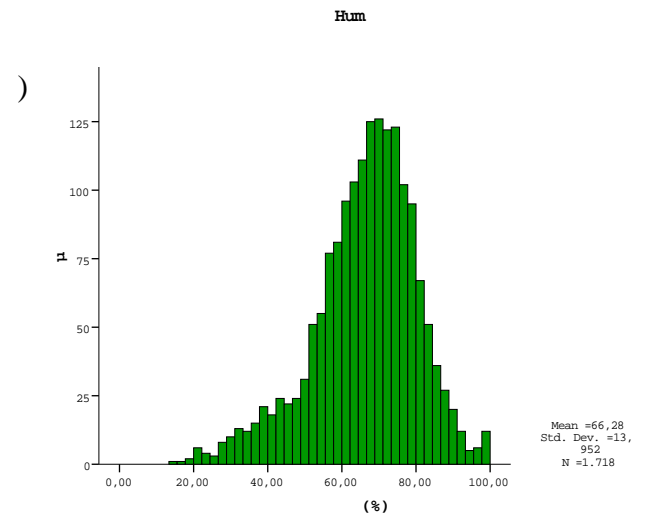
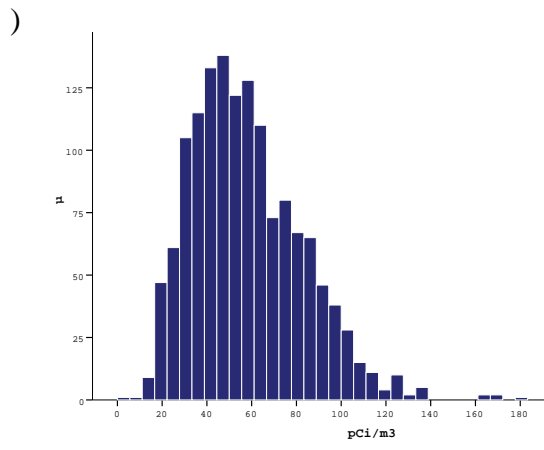


21.

pCi/m³, % , m/s , ppb_v , °C
 (UTC+2 Coordinated Universal Time). HYSPLIT

μ		μ /
²²² Rn	01/07/01-31/12/06	(), μ .
O ₃	01/01/01-31/12/06 21/07/01-31/12/06	μ , μ -
μ	21/07/01-31/12/06	.
μ	01/01/02-31/12/06	
.	21/07/01-31/12/06	

12.



22. $\mu\mu$ μ μ
 (%) (ppbv,) μ
 (Watt/m²) (C) (pCi/m³),)
 2001-2006. μ (m/s),)

pCi/m ³	2003				
		μ			
	19,40	22,70	19,40	33,50	22,30
	129,10	47,90	86,70	129,10	110,40
μ					
10%	29,76	22,98	22,71	44,42	32,20
25%	41,45	26,55	29,28	55,98	43,20
50%	59,15	34,60	37,75	67,40	68,90
75%	79,08	45,25	52,83	80,55	88,00
90%	96,84	47,50	75,60	99,09	98,10

16. μ pCi/m³. μ 2003 μ

pCi/m ³	2004				
		μ			
	13,60	13,60	16,70	34,00	18,50
	137,40	96,50	69,70	100,40	137,40
μ					
10%	30,62	26,60	24,82	46,60	31,53
25%	40,75	33,00	34,80	55,05	40,85
50%	54,10	46,70	45,60	69,20	56,25
75%	70,30	55,90	55,10	79,85	82,83
90%	88,00	69,30	63,16	89,80	109,61

17. μ pCi/m³. μ 2004 μ

pCi/m ³	2005				
		μ			
	20,70	20,70	20,70	28,90	29,40
	136,40	104,70	96,70	106,10	136,40
μ					
10%	30,73	27,96	29,66	38,46	46,87
25%	39,25	30,70	36,40	49,53	56,70
50%	54,80	39,00	43,40	62,30	70,40
75%	72,60	58,90	55,10	79,58	89,30
90%	87,45	75,52	71,08	86,78	113,82

18. μ pCi/m³. μ 2005 μ

2004, 2006, 2005

3.4.4.

2004, 2005, 2006

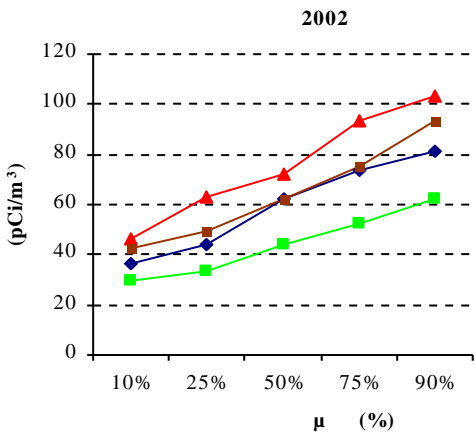
137,40 pCi/m³, 18,50 pCi/m³, 113,62 pCi/m³

90% (2002, 2003, 2006, 2004 (mixed))

109,61 pCi/m³

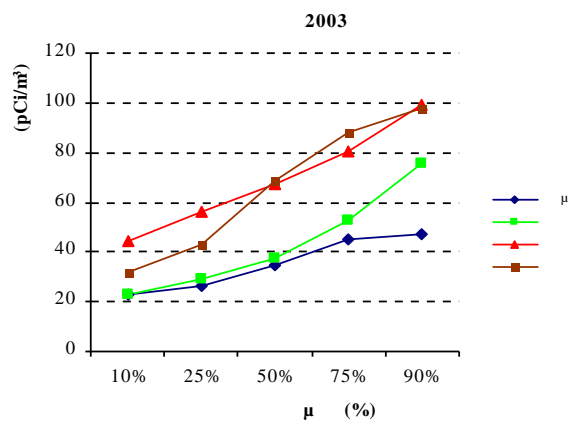
3.5.

2002 (23), 20,72 pCi/m³, 6,88 pCi/m³, 0,05 pCi/m³, 1,90 pCi/m³, 3,73 pCi/m³, 18,07 pCi/m³



23.

μ 2002.

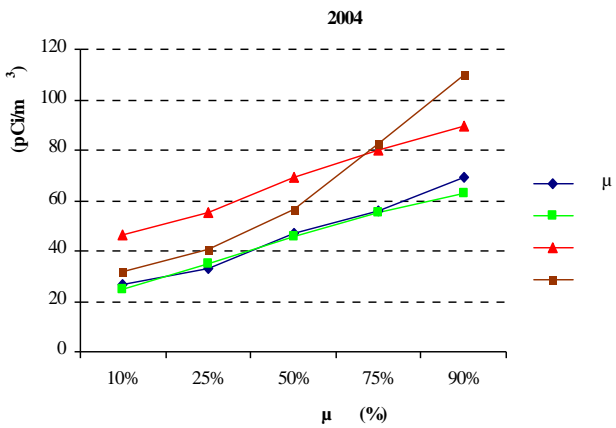


24.

μ 2003.

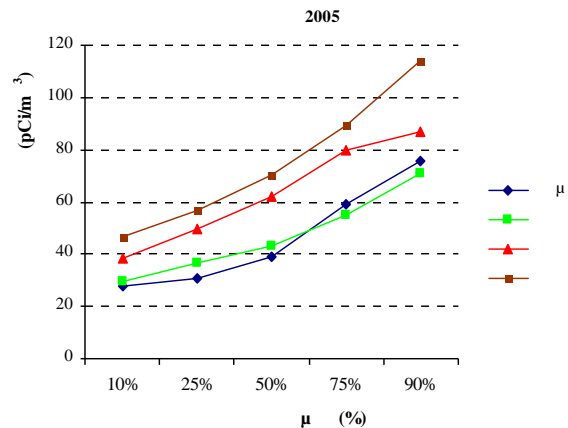
2003 (24), 28,10 pCi/m³

μ μ
 12,22 pCi/m³ 12,78 pCi/m³
 1,5 pCi/m³-7,5 pCi/m³ μ μ



25.

μ
 2004.



26.

μ
 2005.

2004 (25)

μ μ μ μ μ μ μ μ
 μ μ μ μ μ μ μ μ
 6,71 pCi/m³ 46,45 pCi/m³.
 90% 12,95 pCi/m³ 15,07
 pCi/m³ μ 19,81
 pCi/m³ μ



27.

μ
 2006

2004 (26)
 2005 μ μ
 1,70 pCi/m³ 5,70
 pCi/m³ μ
 3,80 pCi/m³
 4,44 pCi/m³ μ
 24,48 pCi/m³, 8,80 pCi/m³
 2005
 15,38 pCi/m³ 30,88 pCi/m³.

10% pCi/m³. 4,30 pCi/m³ 2005 10,88
 -2,72 pCi/m³. (2006 12,08
 90%)

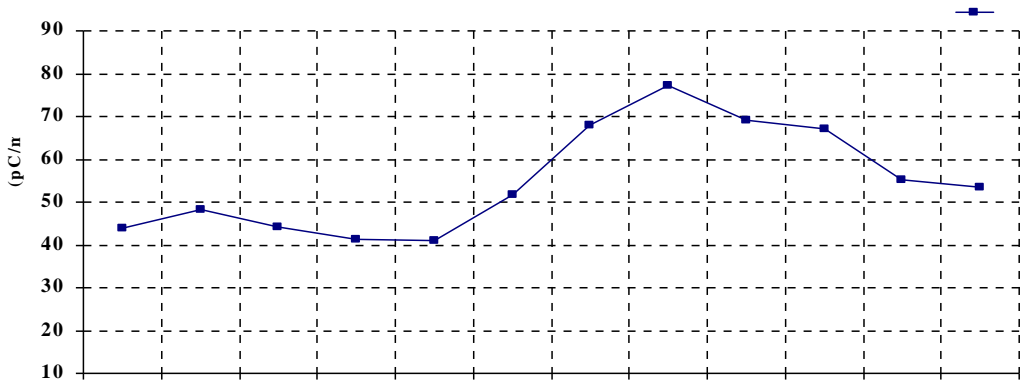
3.6. 2002-2006.

28 pCi/m³ (2002-2006.)
 20 pCi/m³ () 85 pCi/m³ ()
 : 55 pCi/m³ 47 pCi/m³. 55
 2002.

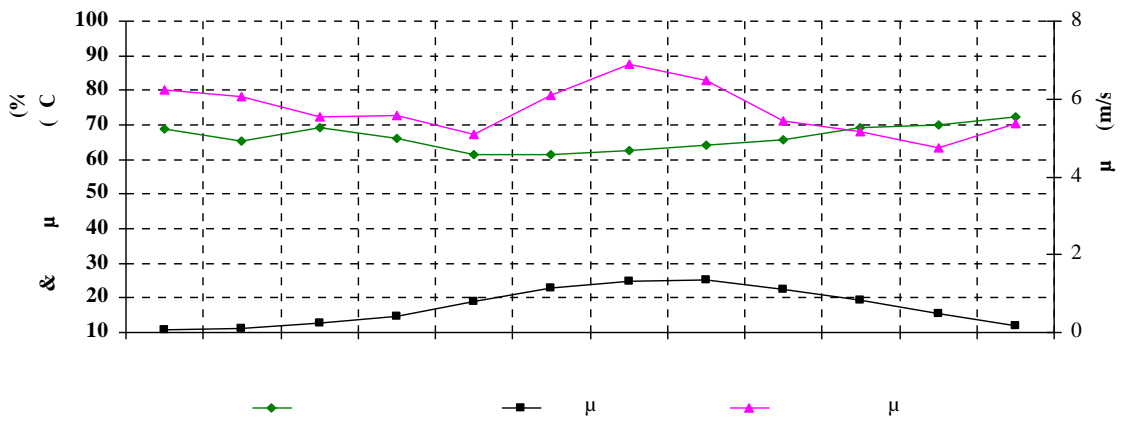
		.		.
	2005	28	2002	10
	2005	23	2002	11
	2006	24	2004	24
	2006	17	2004	19
	2006	20	2005	25
	2006	21	2004	28
	2006	25	2002	20
	2005	20	2003	29
μ	2006	21	2003	26
	2002	5	2005	26
μ	2003	5	2005	20
μ	2005	16	2006	26

20. 2002-2006.

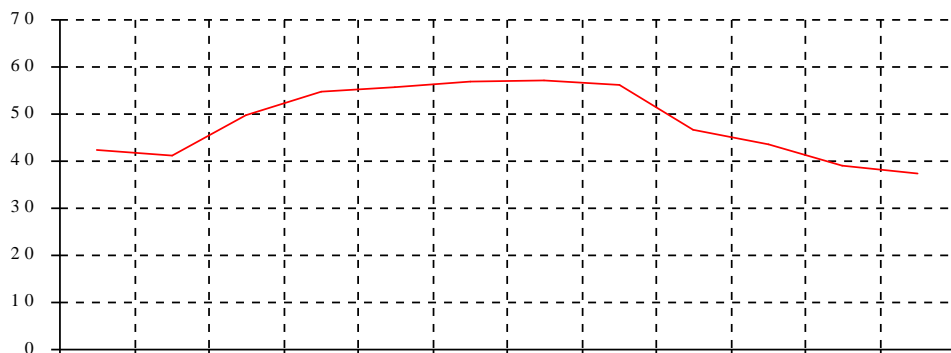
μ μ μ μ μ μ μ μ μ μ μ μ



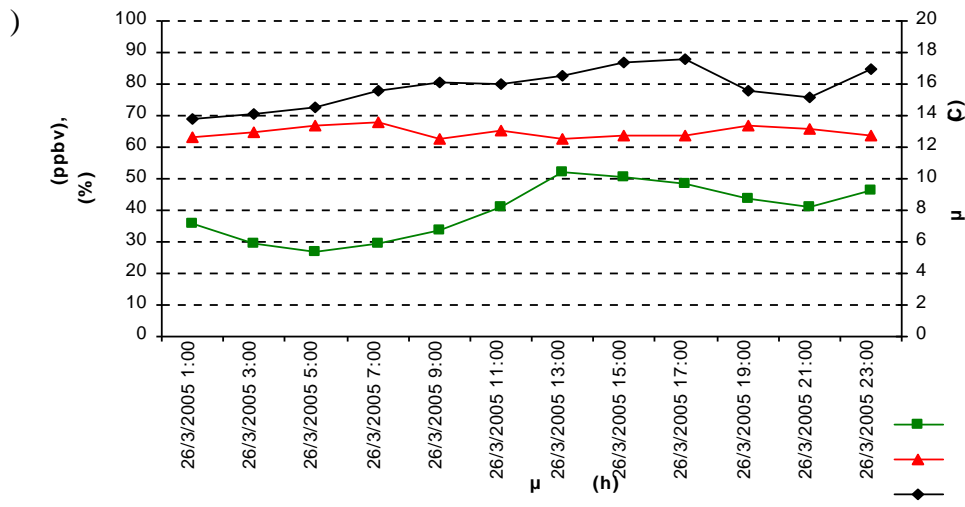
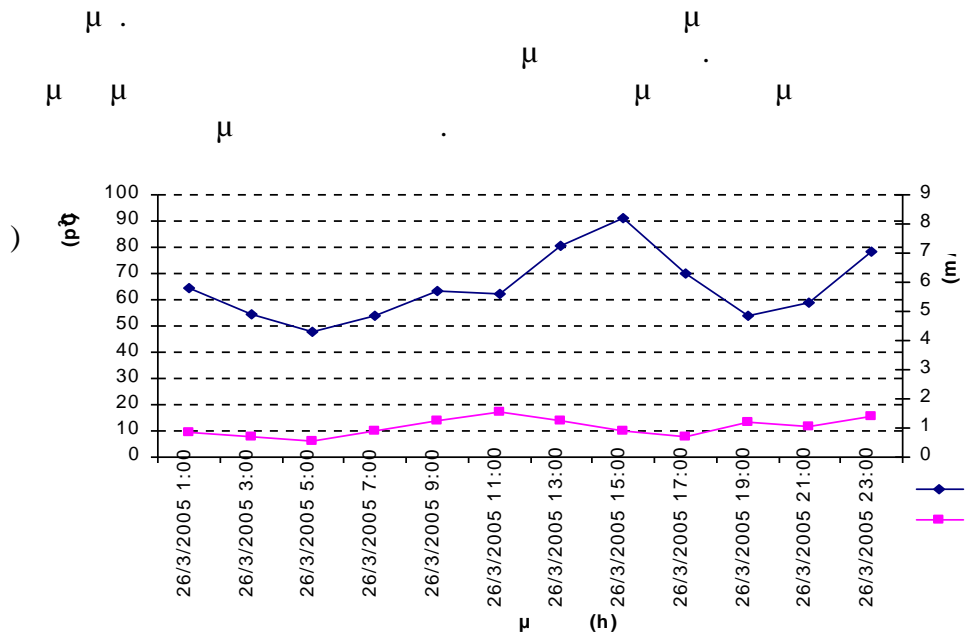
31. μ μ μ 2002-2006.



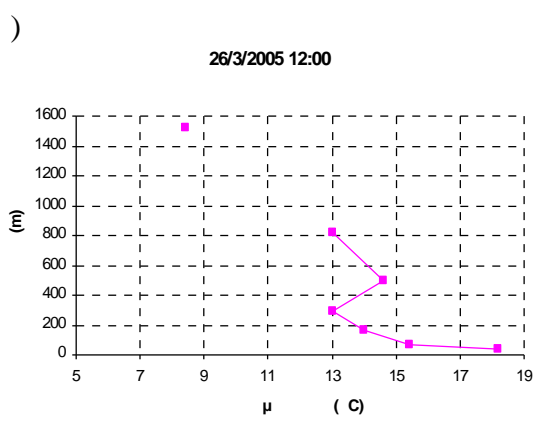
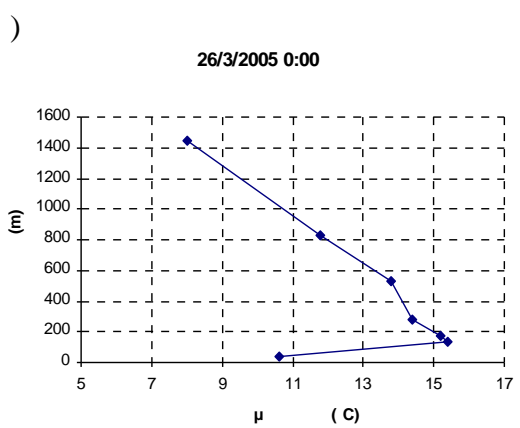
32. μ μ μ μ μ 2002-2006.



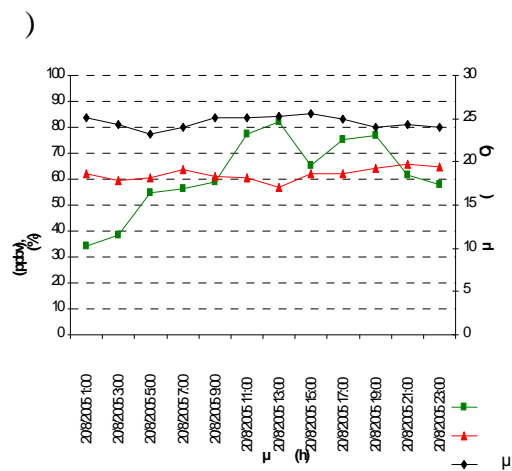
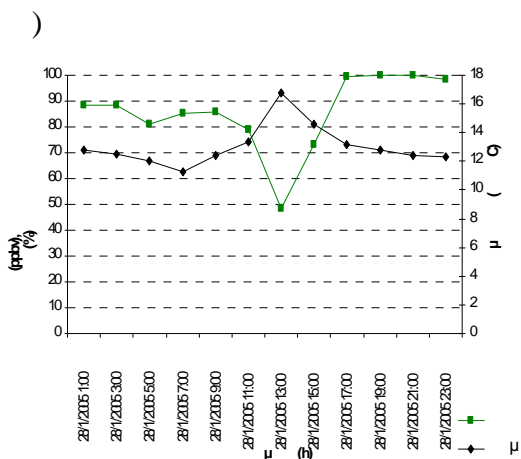
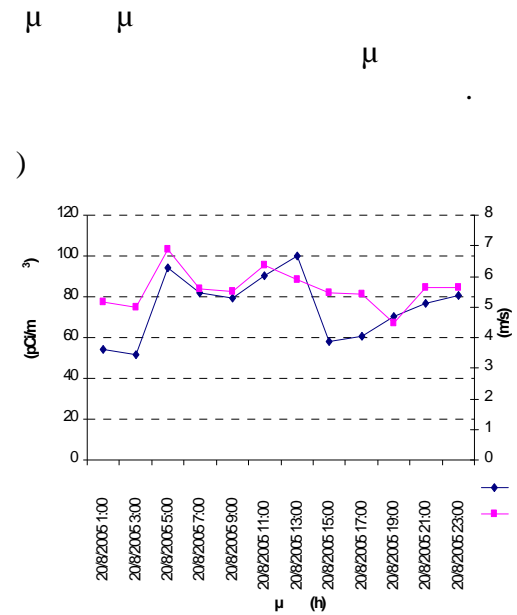
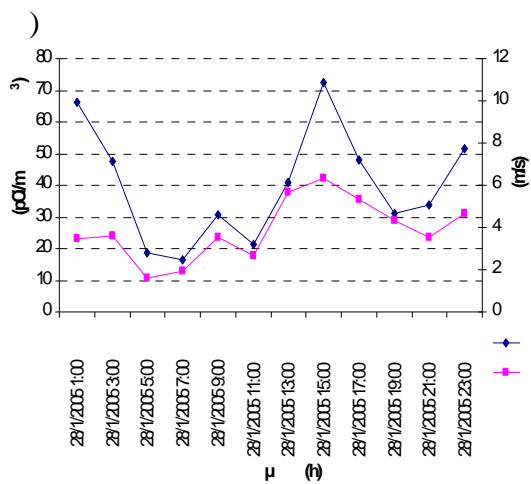
33. μ μ μ 2002-2006.



35.
26/03/2005.



36.
0:00 26/03/2005 12:00.



38.

39.

28/01/2005.

20/08/2005.

20/08/05 (39) µ

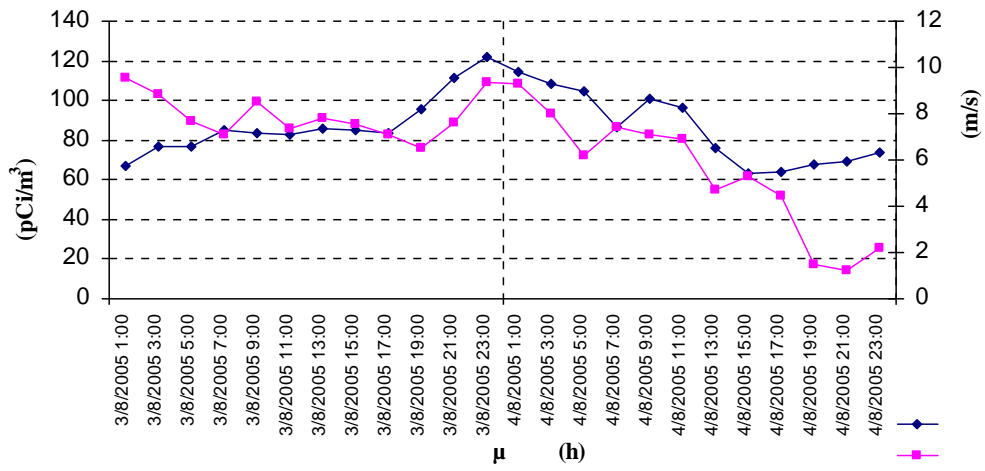
61,6 ppb_v,

75%
2002-2006.

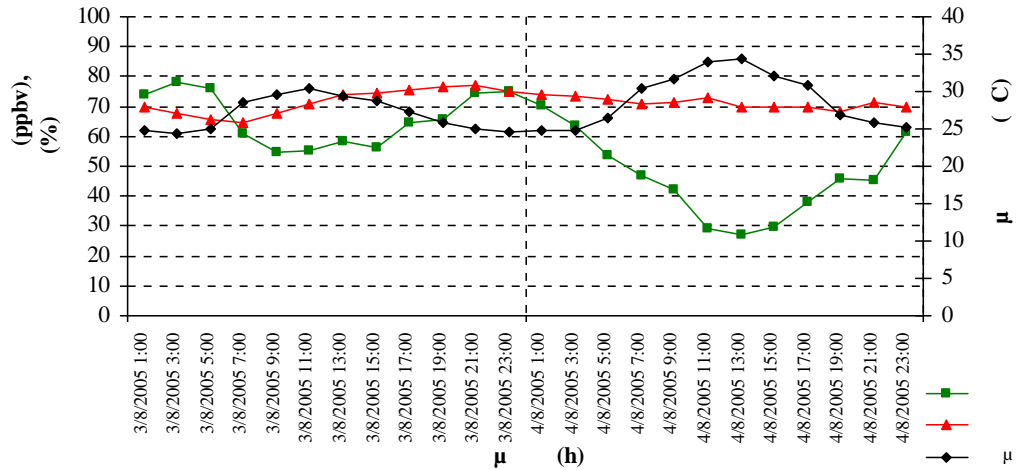
μ .

:

)



)



40.

) μ , μ ,
03/08/2005-04/08/2005.

40

μ μ

μ .

μ

μ . μ

μ μ μ
04/08/2005

0:00

μ . μ
 μ μ

μ
770

μ 23:00

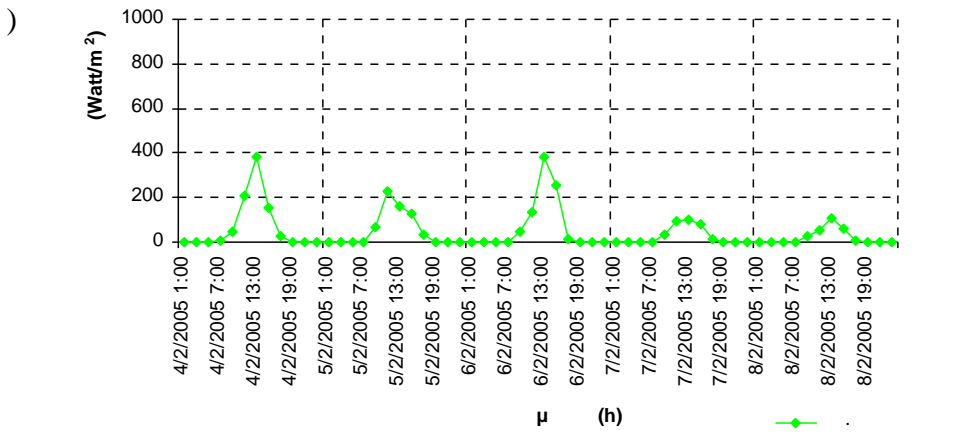
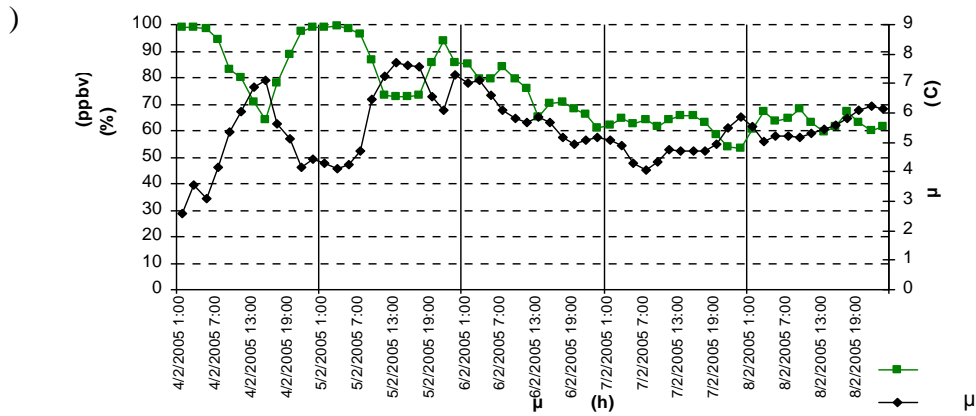
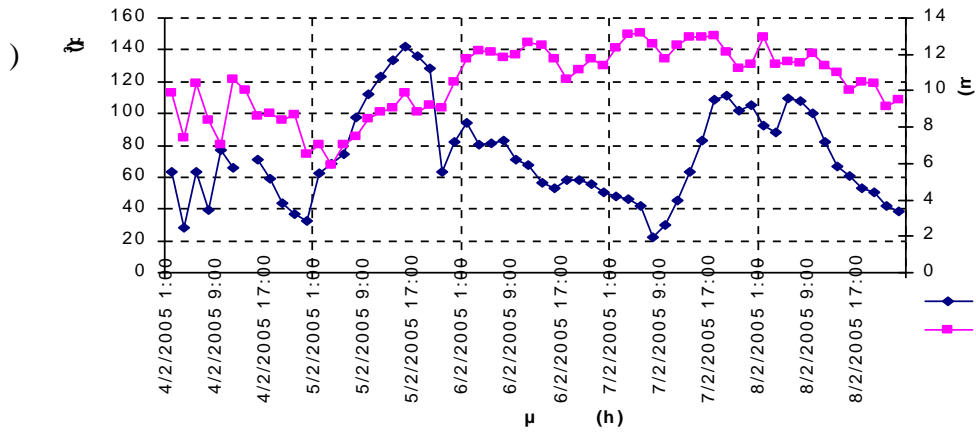
03/08/2005

77,3ppbv

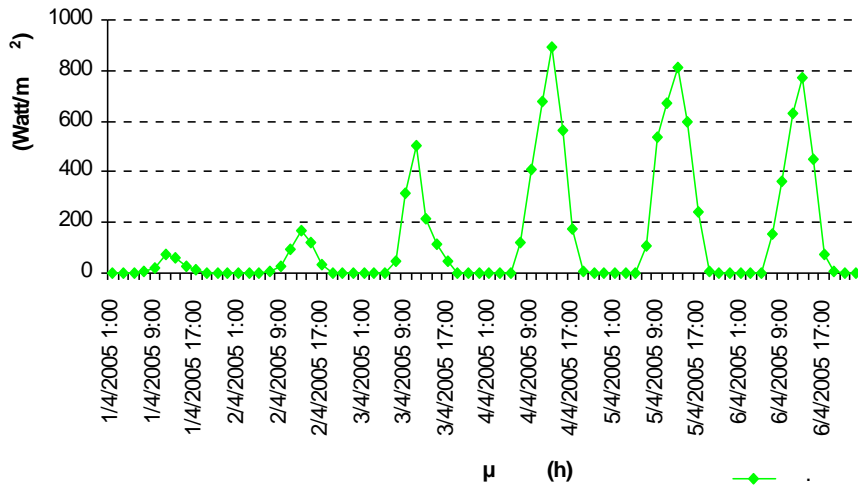
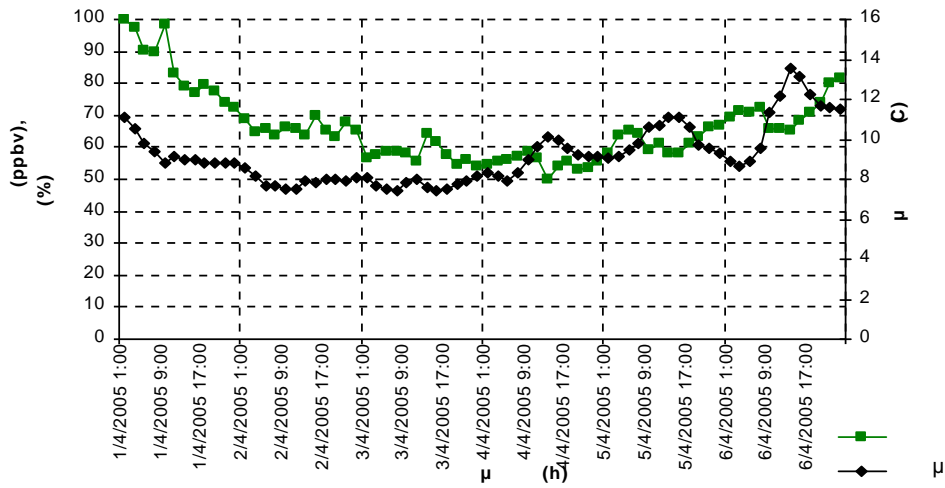
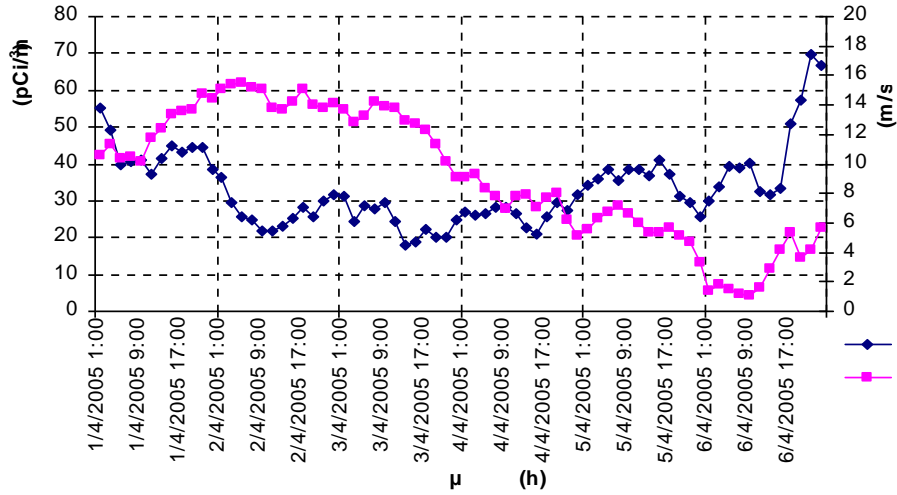
(
 μ μ μ 19:00 μ μ)
 μ 11:00 (μ μ). μ μ μ μ μ μ
 03/08/09 (μ 71,1 ppb_v 03/08/09 μ 71,6 ppb_v
 2002-2006).

3. μ μ

04/02/05 08/02/2005 (41).



41.)
 μ 04/02/2005 08/02/2005.)
 μ ,)



42.

μ

)

μ

μ

01/04/2005-06/04/2005.

4.2.

μ .

μ

μ

μ

43

2006

2002-

μ μ
μ

μ μ
μ

μ μ

μ μ

μ μ

μ ,

2002

μ

2002 (

pCi/m³

2005 μ 7,26 pCi/m³,

2003 μ

) μ μ
9,63 pCi/m³,
9,47 pCi/m³,

2004 μ 6,88
2006 μ 6,30 pCi/m³.

2006

μ

μ μ

μ

μ μ

μ

μ μ

μ

μ

(μ 17:00)

μ , μ
μ

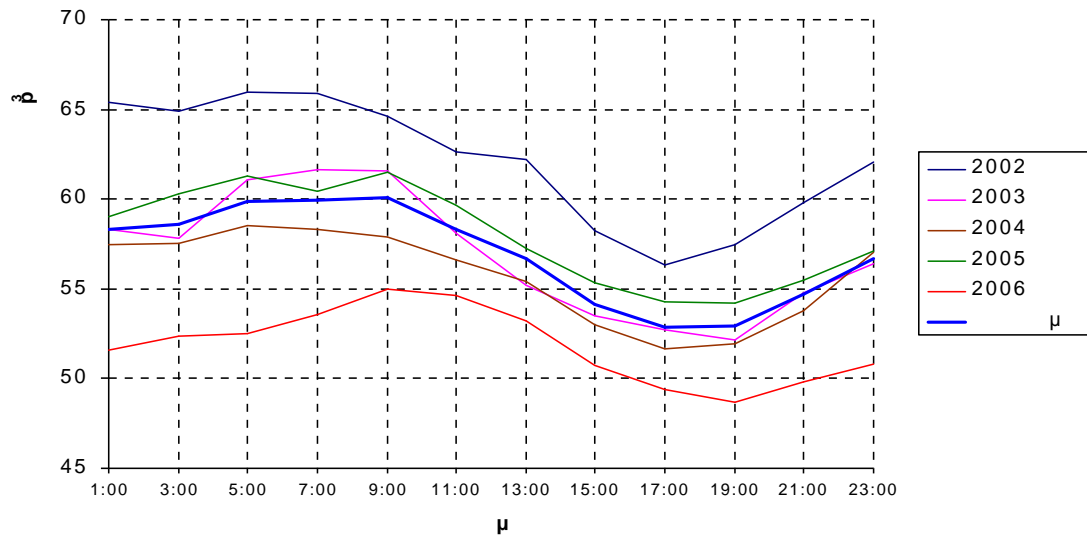
μ 1

(34)

μ

μ

μ .



43.

2006 μ

μ

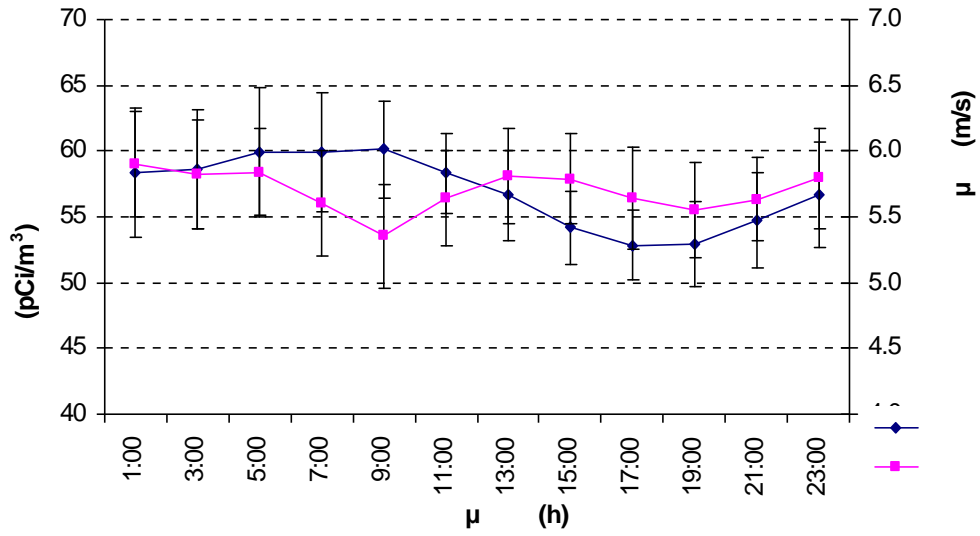
μ

μ

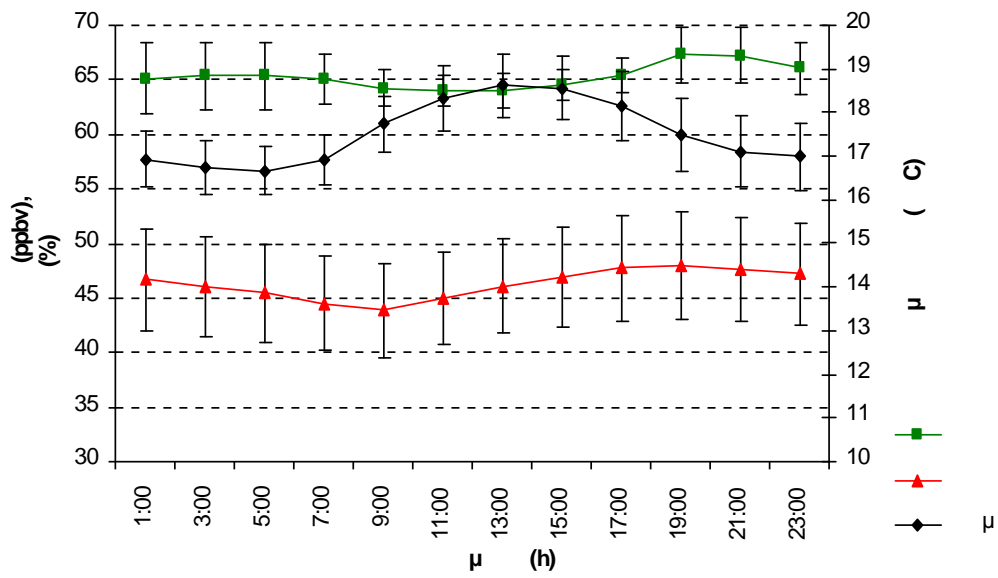
μ

μ

2002-

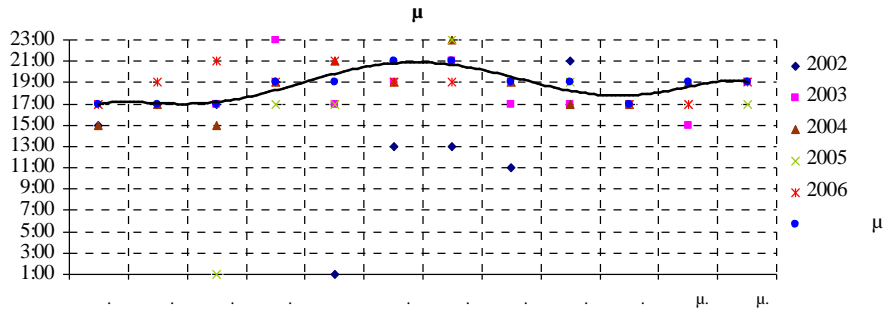


44. μ μ μ

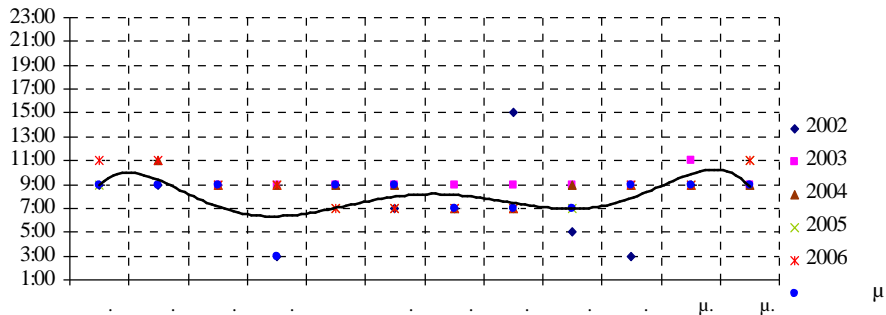


45. μ μ μ

)



)



47.

μ μ μ) μ

47

(UTC+2).

μ μ 17:00 21:00 μ μ μ μ μ μ 7:00

46

4.3.

μ μ μ .

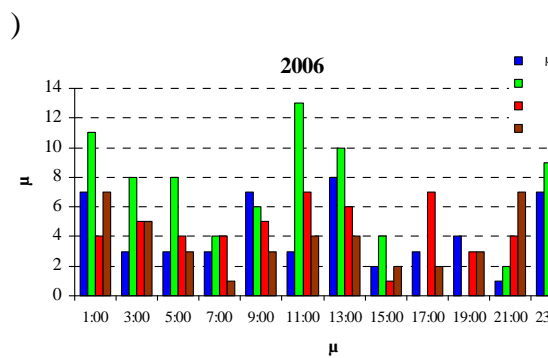
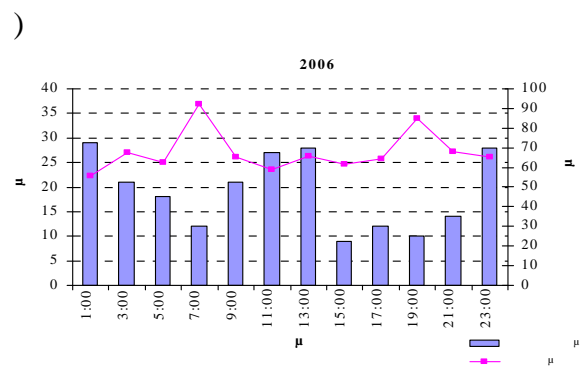
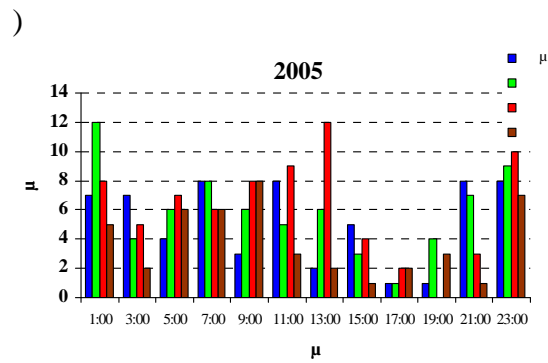
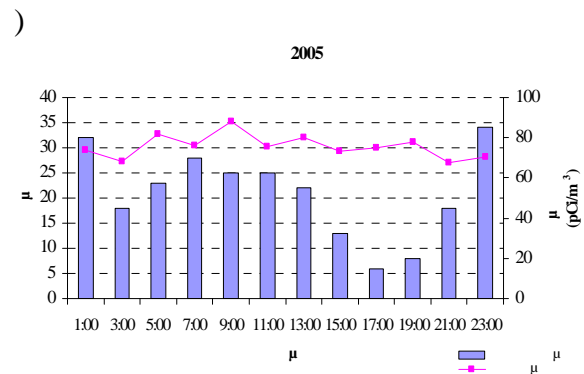
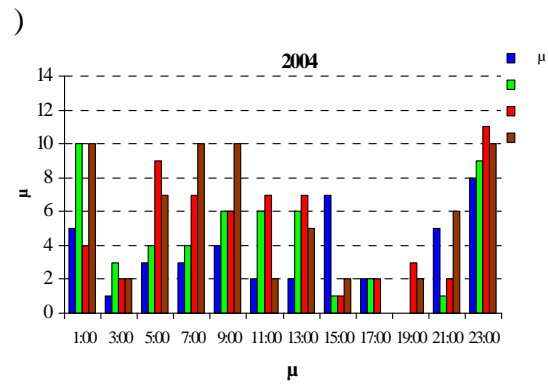
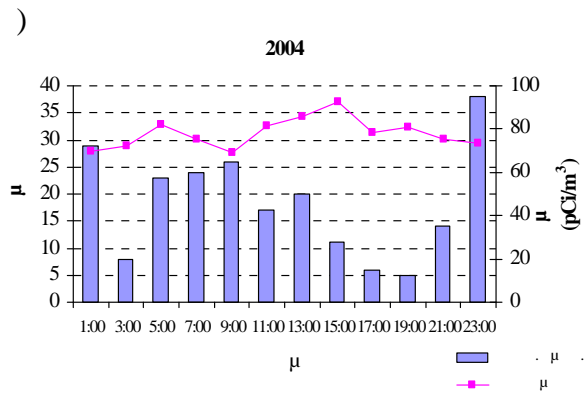
46

4.3.1.

μ μ μ

2004:

(23:00 1:00)
 15:00. 9:00 5:00 7:00 11:00, 13:00
 15:00. 2004 (mixed) /



52.

2004-2006.

2005

μ :

μ 5:00, 9:00
 13:00. μ
 μ 13:00. μ μ
 13:00 μ μ μ 9:00
 μ μ μ 90,7 pCi/m³. μ μ
 μ μ μ 88 pCi/m³. μ μ
 μ μ μ 2 m/s (Pasquill).
 μ 9:00.

2006

μ :

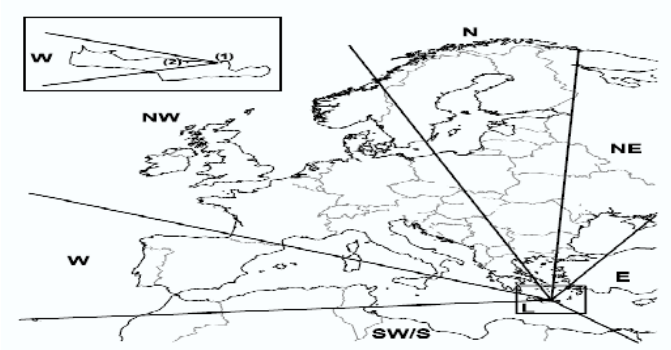
μ 1:00 3:00, 5:00,
 11:00 13:00. μ μ
 2006 , 2006
 2006 . μ μ 13:00 μ μ μ
 2006. μ μ μ μ μ μ ,
 μ μ μ μ μ (μ μ) , μ
 μ μ μ μ , μ

4.4.

μ μ .

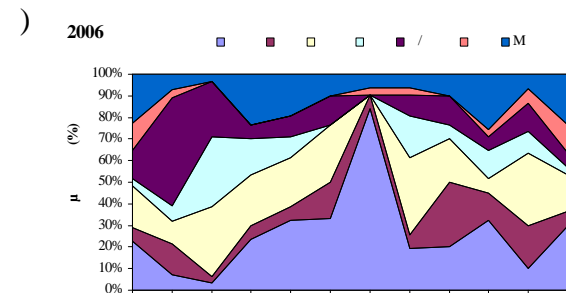
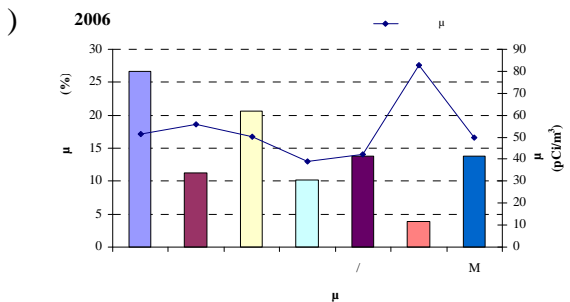
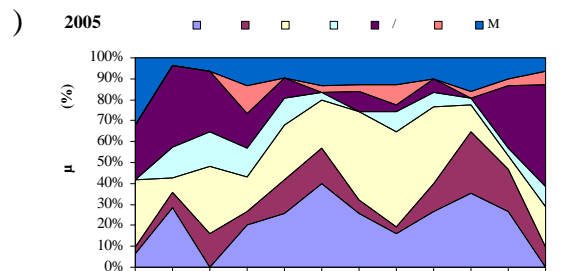
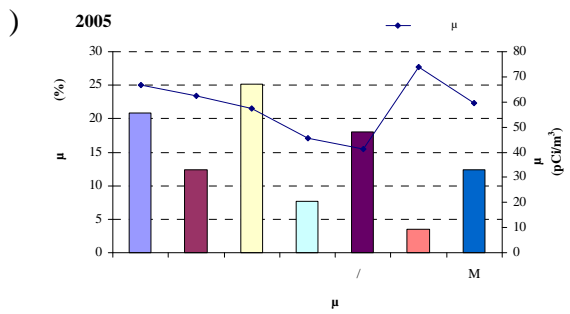
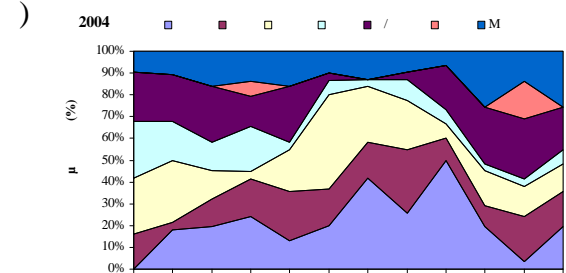
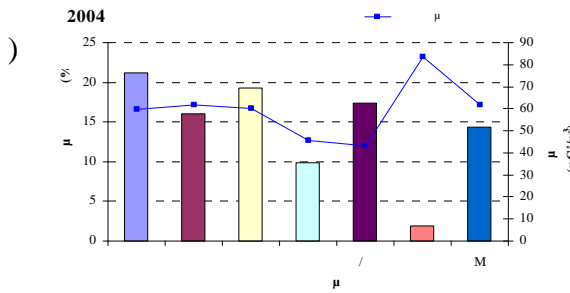
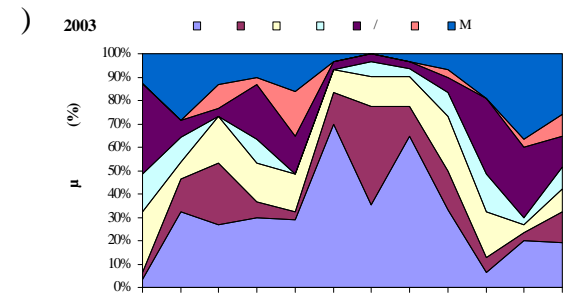
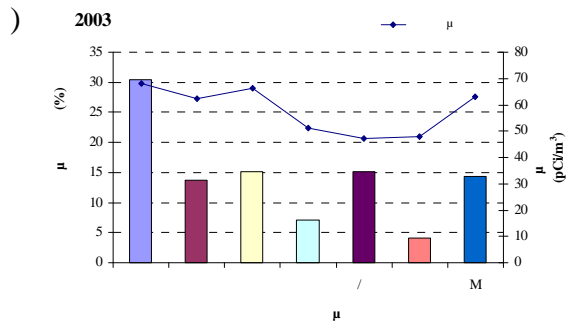
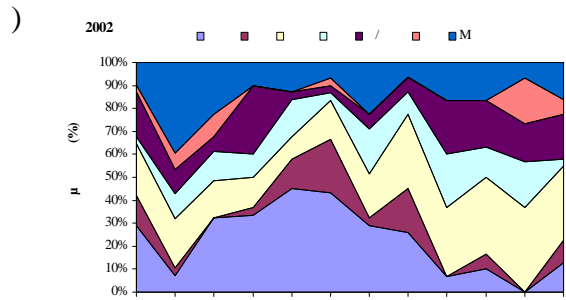
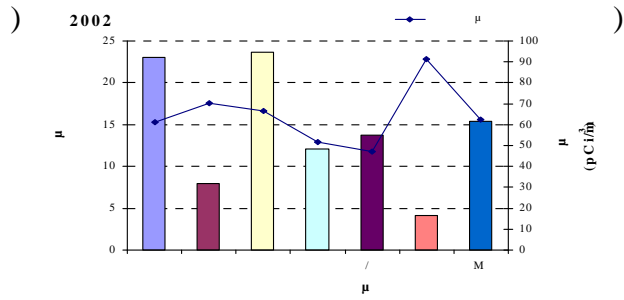
HYSPLIT NOAA

μ μ μ μ μ μ
 μ μ μ μ 2002-2006. μ μ
 μ μ (μ 53) μ μ
54 55. μ μ .



53.

μ .



54. μ

μ μ μ
2002-2006. (, , , ,)
,).

55. μ

μ μ μ
2002-2006 (, , , ,).

60 pCi/m^3
 54 (, , , ,) μ

55 () μ
 μ

(, , , ,)
 μ

(μ
 $\mu \mu \mu$) μ

($\mu \mu \mu$).
 $\mu \mu \mu$).

4.4.1. μ

30 pCi/m^3
 50 pCi/m^3

30 pCi/m^3
 50 pCi/m^3

μ (μ
 μ)
 μ

μ (μ
 $\mu \mu \mu$) μ

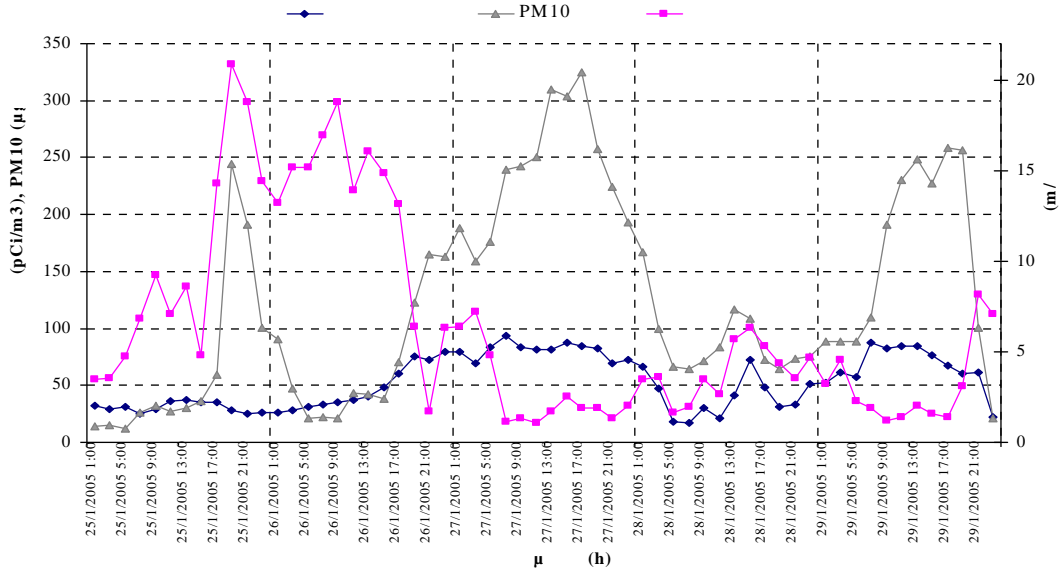
μ
 μ

^{222}Rn
 μ

4.4.1.1. PM_{10}

PM_{10}
 PM_{10}

PM_{10}
 PM_{10}



56. μ 25/01/2005 29/01/2005 , 10 μ .

μ μ μ 25/01/2009-29/01/2009 μ /

μ μ μ PM₁₀ (**56**). μ μ

μ μ μ μ PM₁₀.

μ . μ μ μ

10 (25/01/2005 19:00).

27/01/2005 μ μ μ μ

4.4.2. μ .

μ μ 10% .

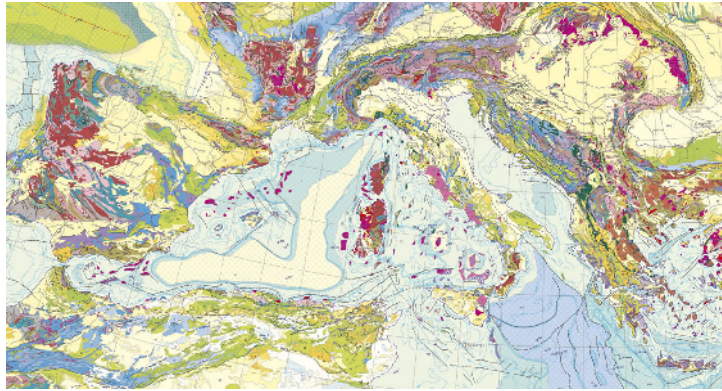
30pCi/m³ , 50pCi/m³ . μ μ μ 50pCi/m³

μ μ μ (<3 m/s). μ μ

μ μ μ μ μ

μ μ μ μ μ

μ μ μ μ μ



57.

<http://www.bgr.de/karten/IGM E5000/IGME5000.htm>.

μ . μ
4.4.3. μ .
 μ μ μ μ
 μ μ 20% 30%. μ μ μ
 μ μ μ 50 pCi/m³. μ
 μ μ μ μ 3 μ , . μ
 μ (04/02/2005-08/02/2005). μ
 μ μ μ .

4.4.3.1. *PM₁₀*

$\mu\mu$ μ μ μ 04/02/2005
 08/02/2005 (**58**).
 μ μ μ
 10 $\mu\text{gr}/\text{m}^3$ μ μ μ μ μ μ
 17 $\mu\text{gr}/\text{m}^3$. μ μ μ μ μ μ
 52,8 pCi/m³ μ μ μ μ μ μ
 102 pCi/m³.

4.5.

μ

μ

μ μ μ , μ , μ μ ,
 μ μ μ μ 2.2 μ μ μ μ ,
 μ μ , μ μ μ μ μ μ ,
2002-2006 .

μ

μ

μ

μ

(Washington and Rose 1990, Pearson, 1965)

μ

μ

μ

μ

2006

μ

μ

μ

(

2002-2003

μ

μ

μ

μ

μ

μ

)

2006

μ

μ

,

μ

μ

μ

μ

2006

μ

μ

2006.

μ

2006

μ

μ

μ

2006

μ

(Luterbacher et al., 2007, G. J. van Oldenborgh, 2007).

μ

μ

μ

μ

μ

61

μ

μ

1961-1990,

μ

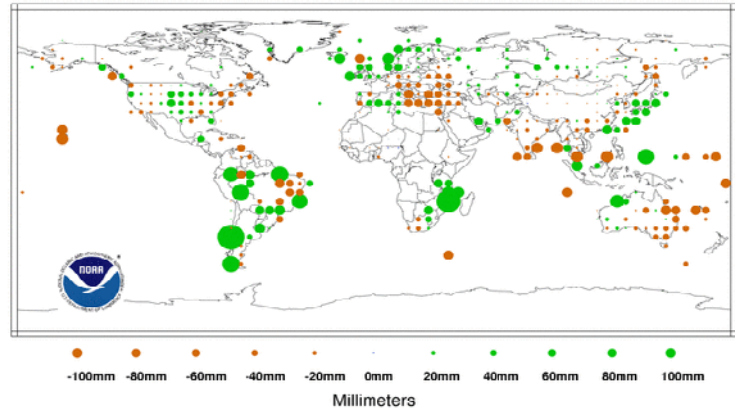
62,

μ

Precipitation Anomalies December 2006

(with respect to a 1961-1990 base period)

National Climatic Data Center/NESDIS/NOAA



61.

(1961-1990) (

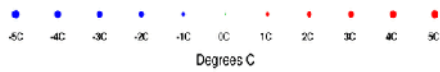
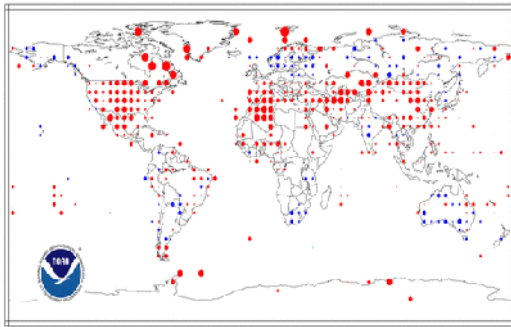
: <http://www.ncdc.noaa.gov/sotc>).

μ

2006 μ

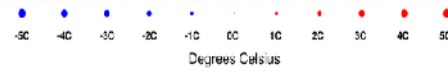
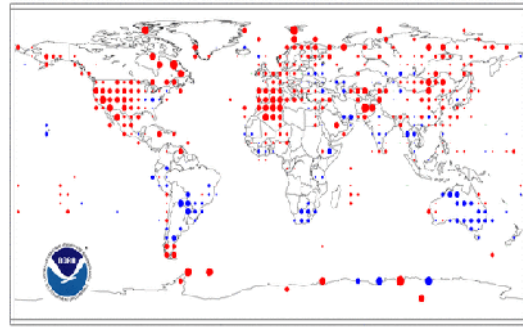
Temperature Anomalies Mar-May 2006

(with respect to a 1961-1990 base period)
National Climatic Data Center/NESDIS/NOAA



May 2006 Temperature Anomalies

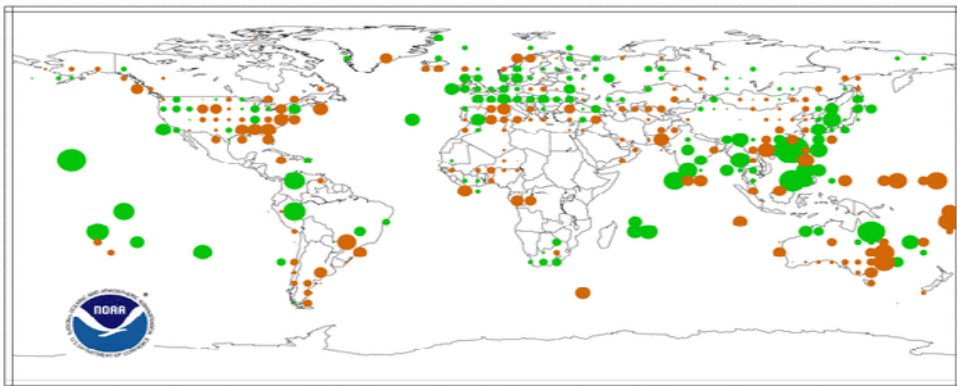
(with respect to a 1961-1990 base period)
National Climatic Data Center/NESDIS/NOAA



64. μ 1961-1990 μ 2006
 μ (: <http://www.ncdc.noaa.gov/sotc>).

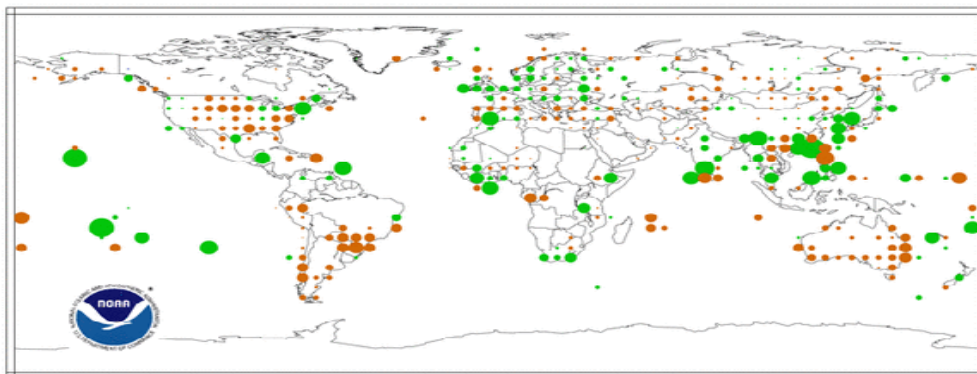
March-May 2006 Precipitation Anomalies

(with respect to a 1961-1990 base period)
National Climatic Data Center/NESDIS/NOAA



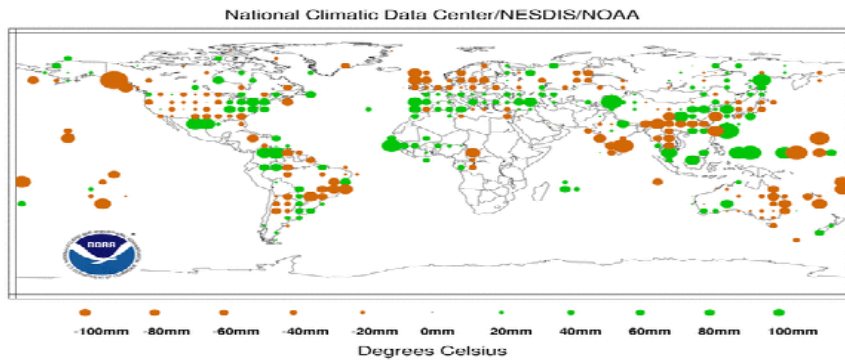
Precipitation Anomalies May 2006

(with respect to a 1961-1990 base period)
National Climatic Data Center/NESDIS/NOAA

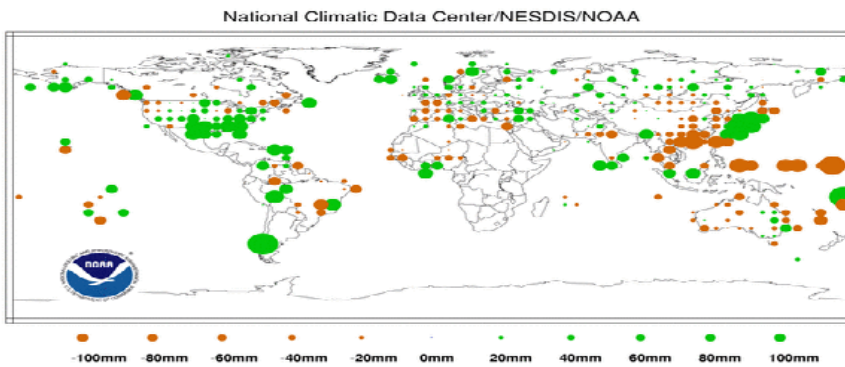


65. μ 2006 μ
 (1961-1990) (: <http://www.ncdc.noaa.gov/sotc>).

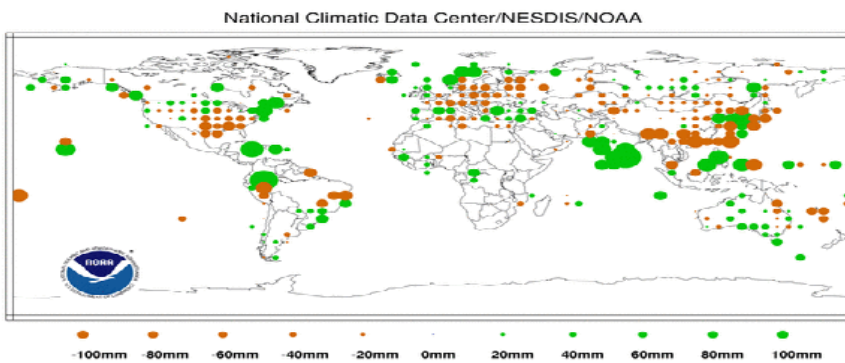
) **Sep-Nov 2003 Precipitation Anomalies**



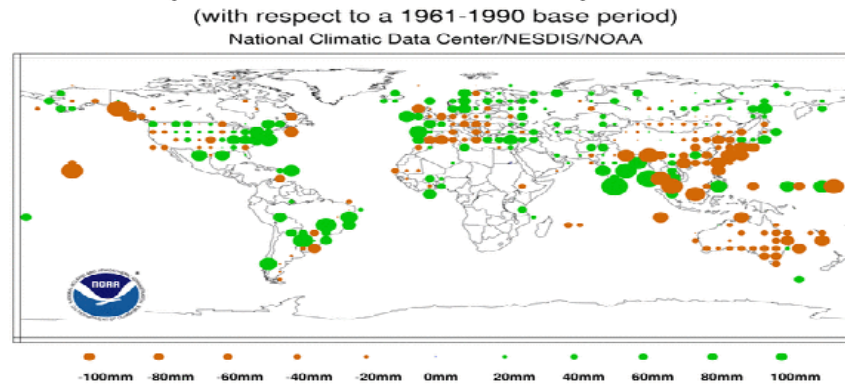
) **Sept-Nov 2004 Precipitation Anomalies**



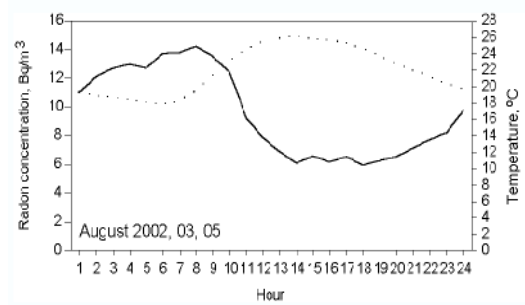
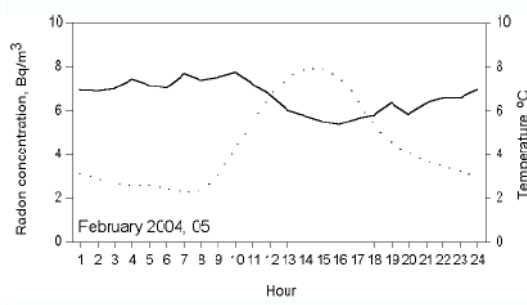
) **Sep-Nov 2005 Precipitation Anomalies**



) **Precipitation Anomalies Sep-Nov 2006**



67.
2003-2006 μ (1961-1990) (: <http://www.ncdc.noaa.gov/sotc>).



69. μ μ
 μ
 μ

(D. Dosideri et al., 2006).

70. μ μ
 μ
 μ

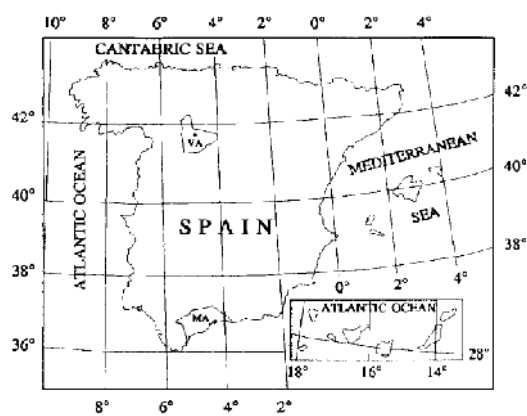
(D. Dosideri et al., 2006).

μ $\mu\mu$
 μ 7 Bq/m^3 ($\sim 216 \text{ pCi/m}^3$)
 $(\sim 270 \text{ pCi/m}^3)$.

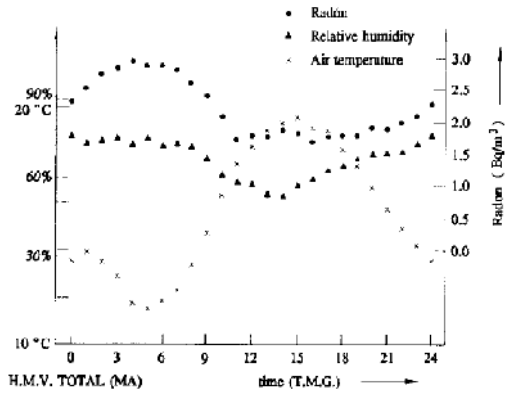
μ μ μ μ
 μ 10 Bq/m^3
 μ μ

4.6.2. (,).

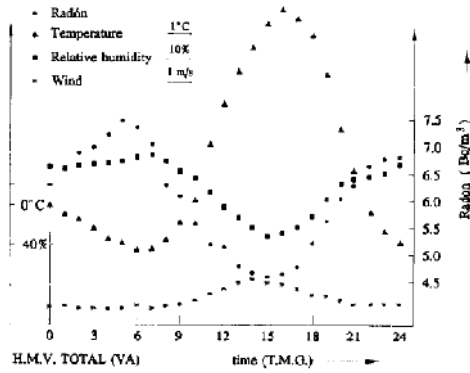
μ μ μ μ
 μ 36 40 30 μ μ : 4 29 58 μ
 μ 41 38 40 μ μ : 4 44 36
 μ 728m μ μ μ μ μ μ
 $2,5 \text{ Bq/m}^3$ ($\sim 67 \text{ pCi/m}^3$) 6 Bq/m^3 ($\sim 162 \text{ pCi/m}^3$).
 μ μ μ μ μ μ
 μ μ μ μ



71. μ μ μ μ
 (, VA) (C. Dueñas et al., 1994)

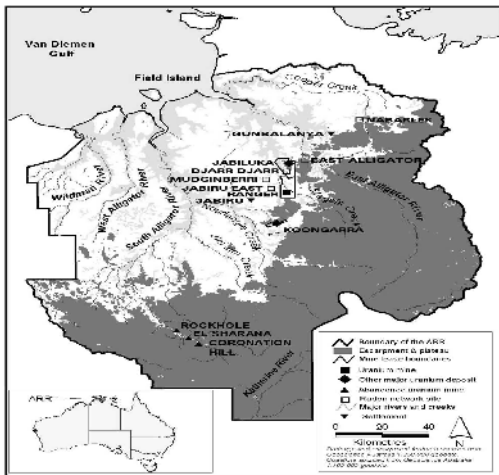


72.



73.

4.6.3. Alligator Rivers Region



74.

Alligator Rivers

Alligator Rivers. Mudginderrri, Djarr Djarr billabong, East Alligator Ranger Station Nabarlek.

Rivers

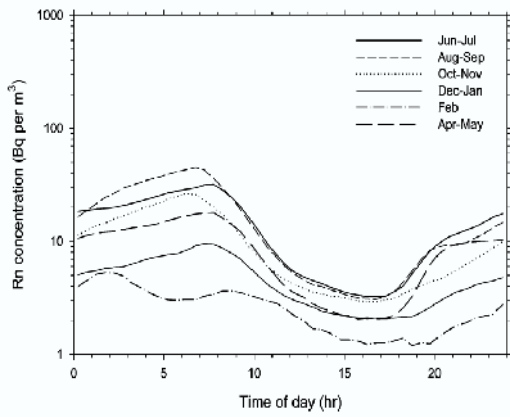
Alligator

Nabarlek

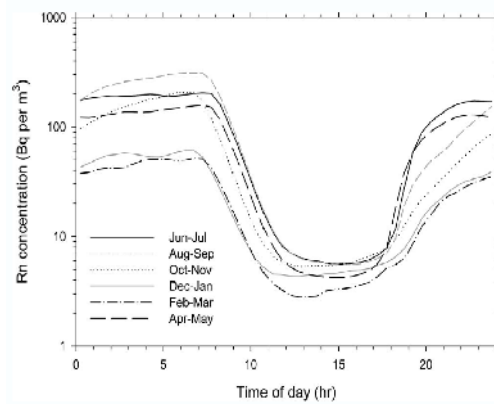
Nabarlek.

Djarr Djarr

Djarr Djarr



75. Nabarlek
1998 1999.



76. Djarr Djarr
1998 1999.

Nabarlek

Djarr Djarr

4.6.4. Hok Tsui, Gosan Mauna Loa.

Hok Tsui, Cape D' Anguilar (22 12 , 114 15), Gosan (33 18 , 126 09), Mauna Loa Observatory (19 32,2 , 155 34,7 W)

5065±4640 (~136,89± 125,40 pCi/m³), 2868±1511 (~77,51± 40,84 pCi/m³), 146±97mBqm⁻³ (~3,94± 2,62 pCi/m³), Hok Tsui, Gosan Mauna Loa

77 78.

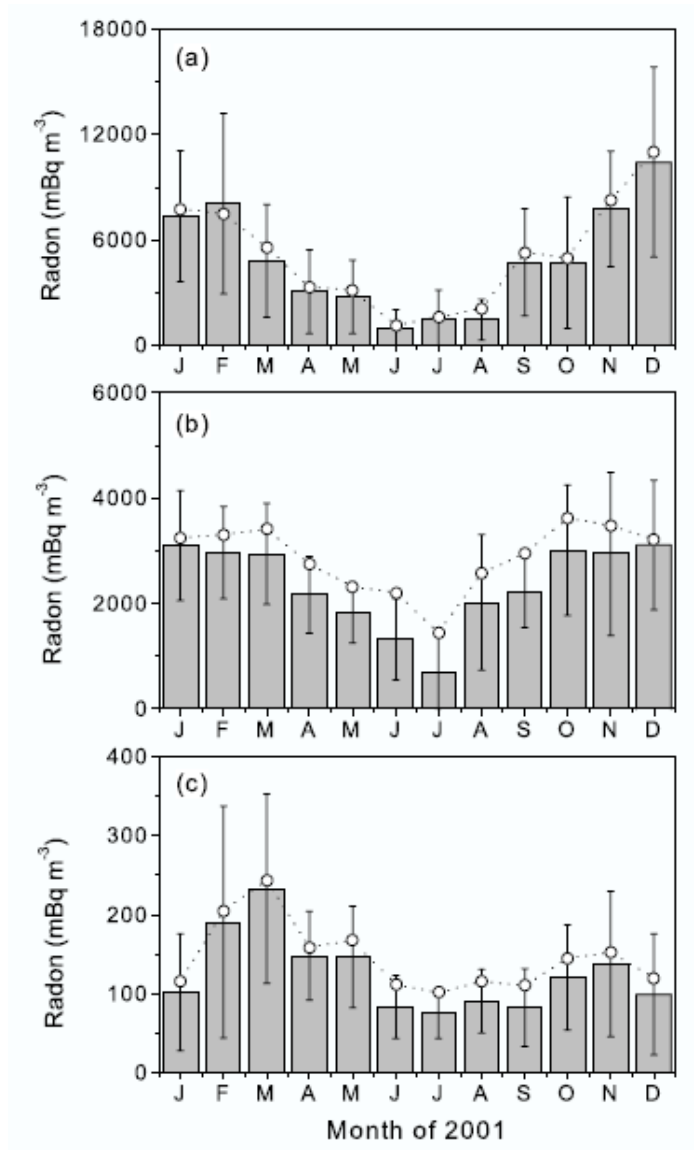
Hok Tsui, Gosan, Mauna Loa

Gosan. 77

μ
 μ

μ . μ
 μ

Gosan.



77.
) Mauna Loa.
 μ

μ

) Hok Tsui,) Gosan

μ

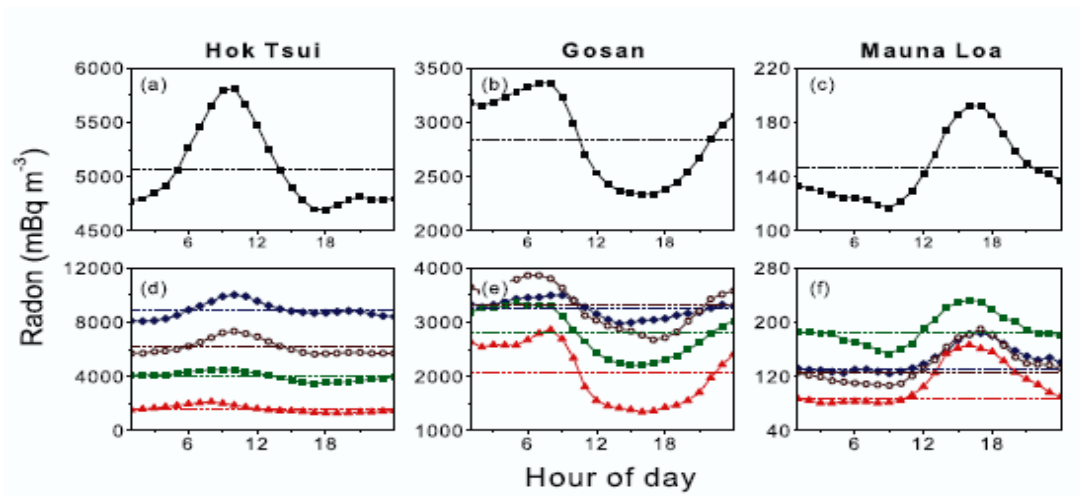
μ

μ

μ

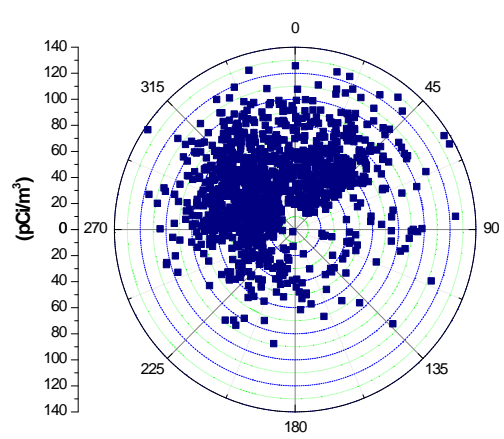
$\mu\mu$

± 1

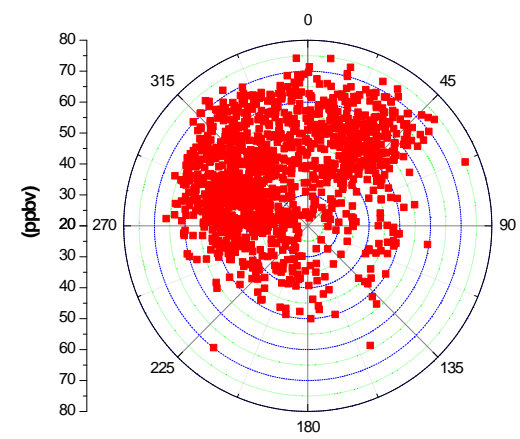


78. (a-c) μ (d-f) $\mu\mu$
 Hok Tsui, Gosan, Mauna Loa, 2001.

79. μ (μ). $\mu\mu$
 μ μ μ μ , , , μ
 μ μ μ μ μ μ
 μ (μ 0-45 μ). $\mu\mu$
 μ μ μ μ μ .



79. μ 2002-2006.



80. μ 2002-2006.

5. SPSS.

5.1. (Simple Linear Regression).

X_i (explanatory variable) Y_i (dependent variable)
 Y_i (response variable)

$$Y_i = b_0 + b_1 X_i + \epsilon_i, \quad i = 1, 2, 3, \dots, n \quad (.1)$$

b_0, b_1 (intercept), ϵ_i (error term), $i = 1, 2, \dots, n$
 b_0 (intercept), b_1 (slope), b_1 (regression coefficient).

$$\hat{b} = \frac{S_{XY}}{S_{XX}}, \quad \hat{b}_0 = \bar{Y} - \hat{b}_1 \bar{X} \quad (.2)$$

$$y = \hat{b}_0 + \hat{b}_1 x \quad (.3)$$

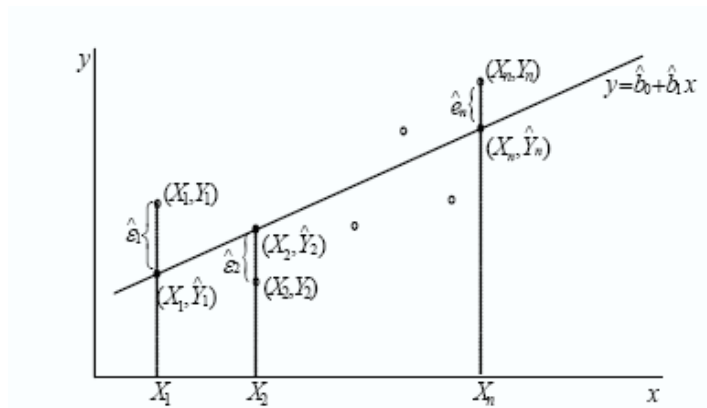
(residual). $\hat{\varepsilon}_i = Y_i - \hat{Y}_i$

$$\hat{\sigma}^2 = \frac{1}{n} \sum_{i=1}^n (Y_i - \hat{b}_0 - \hat{b}_1 X_i)^2 \quad (.4)$$

(SST) (SSR) (SSE)

$$R^2 = \frac{SSR}{SST} = \frac{SST - SSE}{SST} \quad (.5)$$

SST, SSR, SSE Sum of Squares Total, Sum of Squares Regression, Sum of Squares Error. R^2



81. (Boutsikas M.V., 2004).

$Y' = \sqrt{Y}$, $Y' = \ln Y$, $Y' = 1/Y$, $X' = \sqrt{X}$, $X' = \ln X$, $X' = 1/X$

$$Y' = \sqrt{Y}, Y' = \ln Y, Y' = 1/Y, X' = \sqrt{X}, X' = \ln X, X' = 1/X \quad (.6)$$

F-test. F-test : $b_1=0$.

F test
$$F = \frac{MSR}{MSE} = \frac{SSR}{SSE/(n-2)} \quad (.10)$$

SSR : Sum of Squares Regression, SSE: Sum of Squares Error (n -2)

SSE **10,**
0: $b_1 = 0$ (Boutsikas M.V., 2004).

5.3.

SPSS

μ (C)	18,70 (+) 99%	3,70 (-) 95%	2,80 (-) 95%	15,30 (+) 99%	5,40 (-) 99%
(%)	6,00 (+) 99%	30,00 (+) 99%	13,00 (+) 99%	-	12,00 (+) 99%
μ (m/s)	0,60 (-) 95%	6,60 (-) 99%	14,50 (-) 99%	4,20 (-) 99%	1,50 (-) 95%
(Watt/m ²)	8,50 (+) 99%	3,80 (+) 95%	-	1,30 (+) 95%	8,10 (+) 99%
(pbbv)	4,30 (+) 99%	5,10 (+) 95%	-	-	20,80 (+) 99%
(μ)	10,60 (-) 99%	12,90 (-) 99%	15,30 (-) 99%	1,70 (-) 95%	12,70 (-) 99%
. (m)	4,90 (-) 99%	5,10 (-) 95%	7,00 (-) 99%	10,20 (-) 99%	3,50 (-) 99%

25.

	μ	μ	R^2	F	Sig.
μ	0,593	0,534	0,315	131,66	4.61088E-70
	0,477	0,453			
μ	-0,129	-0,154		Nobs.: 855	

26.

$\mu\mu$

μ

μ

)

μ

μ

μ

27

μ

μ

μ

μ

μ

0,05

F test

μ

μ

μ

μ

μ

μ

$\mu\mu$

μ

μ

μ

μ

μ

,

μ

μ

μ

μ

μ

μ

μ

μ

:

$$^{222}Rn = (-0,23 \pm 0,031) \cdot \mu + (52,68 \pm 3,22) \cdot (\mu \cdot 12)$$

$$+ (0,33 \pm 0,06) \cdot \mu + (-0,002 \pm 0,0005) \cdot \mu$$

μ

μ

μ

μ

μ

μ

μ

μ

μ

μ

	μ	μ	R^2	F	Sig.
	-0,265	-0,252	0,139	45,32	4,23825E-27
	0,182	0,189			
	-0,125	-0,121		Nobs.:822	

27.

$\mu\mu$

μ

μ

$$F_i = \sum_{j=1}^p W_{ij} Z_j = W_{i1} Z_1 + W_{i2} Z_2 + \dots + W_{ip} Z_p \quad (i=1, 2, \dots, m \quad j=1, 2, \dots, p) \quad (.13)$$

$$W_{ij} = \frac{F_{ij}}{F_j} \quad (i=1, 2, \dots, m \quad j=1, 2, \dots, p) \quad (.14)$$

$$z_j = \alpha_{j1} F_1 + \alpha_{j2} F_2 + \dots + \alpha_{jm} F_m + U_j \quad (j=1, 2, \dots, n) \quad (.14)$$

$$F_j = \alpha_{j1} F_1 + \alpha_{j2} F_2 + \dots + \alpha_{jm} F_m + U_j \quad (j=1, 2, \dots, n)$$

6.2.1.

$$z_j = \alpha_{j1} P_1 + \alpha_{j2} P_2 + \dots + \alpha_{jn} P_n \quad (j=1, 2, \dots, n) \quad (.15)$$

$$1 = \alpha_{j1}^2 + \alpha_{j2}^2 + \dots + \alpha_{jn}^2, \quad (j=1, 2, \dots, n) \quad (.16)$$

$\mu_i = \sum_{j=1}^n \left(\frac{\alpha_{ji}}{\lambda_j} \right) z_j$

$$P_i = \sum_{j=1}^n \left(\frac{\alpha_{ji}}{\lambda_j} \right) z_j \quad (.17)$$

$\% \mu_i = \frac{\sum_{j=1}^n \alpha_{ji}^2}{n} \cdot 100 \quad (.18)$

$\% \mu_i = \frac{\sum_{j=1}^n \alpha_{ji}^2}{\sum_{j=1}^n h_j^2} \cdot 100 \quad (.19)$

($\sum_{j=1}^n h_j^2$)

, (Child 1970, Philip et al. 1975)

Guilford (1975) $\pm 0,30-0,40$.

) Guttman Kaiser (Cattell, 1978)
) Cattell (1978)

6.2.2.

Meyer-Olkin (KMO),

$$KMO = \frac{\sum_{i=j} r_{ij}^2}{\sum_{i=j} r_{ij}^2 + \sum_{i=j} \alpha_{ij}^2} \quad (20)$$

(r_{ij} — коэффициент корреляции между переменными i и j).

где α_{ij} — коэффициент корреляции между переменной i и фактором j .
 1. Если значение KMO находится в диапазоне от 0,9 до 1,0, то факторная структура данных является идеальной.

2. Если значение KMO находится в диапазоне от 0,8 до 0,9, то факторная структура данных является хорошей.
 3. Если значение KMO находится в диапазоне от 0,7 до 0,8, то факторная структура данных является удовлетворительной.
 4. Если значение KMO находится в диапазоне от 0,6 до 0,7, то факторная структура данных является сомнительной.
 5. Если значение KMO находится в диапазоне от 0,5 до 0,6, то факторная структура данных является плохой.

6. Если значение KMO находится в диапазоне от 0,4 до 0,5, то факторная структура данных является очень плохой.

7. Если значение KMO находится в диапазоне от 0,3 до 0,4, то факторная структура данных является неприемлемой.
 8. Если значение KMO находится в диапазоне от 0,2 до 0,3, то факторная структура данных является очень неприемлемой.
 9. Если значение KMO находится в диапазоне от 0,1 до 0,2, то факторная структура данных является неприемлемой.

10. Если значение KMO находится в диапазоне от 0 до 0,1, то факторная структура данных является неприемлемой.
 (SA) — коэффициент корреляции между переменной i и фактором j .
 R^2 — коэффициент детерминации.

6.3.

μ

μ

μ

μ
2006.

μ

2004

μ

μ

μ

μ

μ

μ

μ

μ

μ

μ

μ

μ ,

, μ

μ

(μg·m⁻³, n=85)				
	μ			
Acetate	0,033	0,023	0,000	0,111
Propionate	0,007	0,006	0,001	0,039
Formate	0,021	0,017	0,000	0,099
MSA	0,006	0,006	0,000	0,027
Pyruvate	0,002	0,002	0,000	0,007
Cl⁻	1,434	1,179	0,000	4,770
NO₃⁻	1,627	0,712	0,128	3,200
SO₄²⁻	1,081	0,875	0,118	8,000
Oxalate	0,078	0,058	0,008	0,301
HPO₄⁻	0,049	0,036	0,000	0,184
Na⁺	1,325	0,717	0,142	3,369
NH₄⁺	0,171	0,085	0,035	0,441
K⁺	0,071	0,057	0,000	0,290
Mg²⁺	0,181	0,115	0,000	0,538
Ca²⁺	1,224	1,558	0,000	8,964
OC	1,110	1,415	0,015	8,288
EC	0,134	0,128	0,000	0,801
Al	0,393	0,782	0,029	5,059
Ca	1,290	2,843	0,000	18,615
Ti	0,025	0,048	0,001	0,290
V	0,003	0,005	0,000	0,023
Cr	0,006	0,016	0,001	0,126
Mn	0,010	0,019	0,000	0,125
Fe	0,535	1,212	0,002	8,509
Ni	0,002	0,002	0,000	0,011
Cu	0,001	0,002	0,000	0,017
Zn	0,017	0,018	0,000	0,126
Cd	0,000	0,000	0,000	0,000
Pb	0,003	0,003	0,000	0,019
Rn	56,567	23,075	17,809	117,581

28.

μ

($\mu\text{g}\cdot\text{m}^{-3}$, n=85)				
	μ			
Acetate	0,045	0,039	0,000	0,286
Propionate	0,010	0,011	0,000	0,063
Formate	0,040	0,039	0,000	0,226
MSA	0,035	0,027	0,003	0,145
Pyruvate	0,009	0,006	0,000	0,026
Cl⁻	0,075	0,063	0,000	0,344
Br⁻	0,005	0,011	0,000	0,063
NO₃⁻	0,104	0,081	0,000	0,394
SO₄²⁻	4,397	2,298	0,304	10,383
Oxalate	0,113	0,057	0,029	0,258
HPO₄⁻	0,051	0,040	0,008	0,220
Na⁺	0,050	0,102	0,000	0,812
NH₄⁺	1,446	0,737	0,293	3,142
K⁺	0,118	0,093	0,000	0,475
Mg²⁺	0,005	0,017	0,000	0,094
Ca²⁺	0,074	0,220	0,000	1,590
OC	1,839	1,419	0,109	9,456
EC	0,268	0,175	0,000	0,717
Al	0,089	0,095	0,000	0,504
Ca	0,258	0,312	0,000	1,811
Ti	0,018	0,018	0,000	0,122
V	0,005	0,004	0,001	0,017
Cr	0,003	0,002	0,000	0,012
Mn	0,002	0,002	0,000	0,015
Fe	0,063	0,143	0,000	1,018
Ni	0,002	0,001	0,000	0,006
Cu	0,002	0,002	0,000	0,009
Zn	0,012	0,014	0,000	0,091
Cd	0,000	0,000	0,000	0,002
Pb	0,006	0,007	0,000	0,047
Rn	56,567	23,075	17,809	117,581

29.

μ

$\mu \quad \mu \quad \mu$

$\mu \quad \mu$

$, \quad \mu \quad \mu$

μ

$\mu \quad \mu$

μ

82, 83

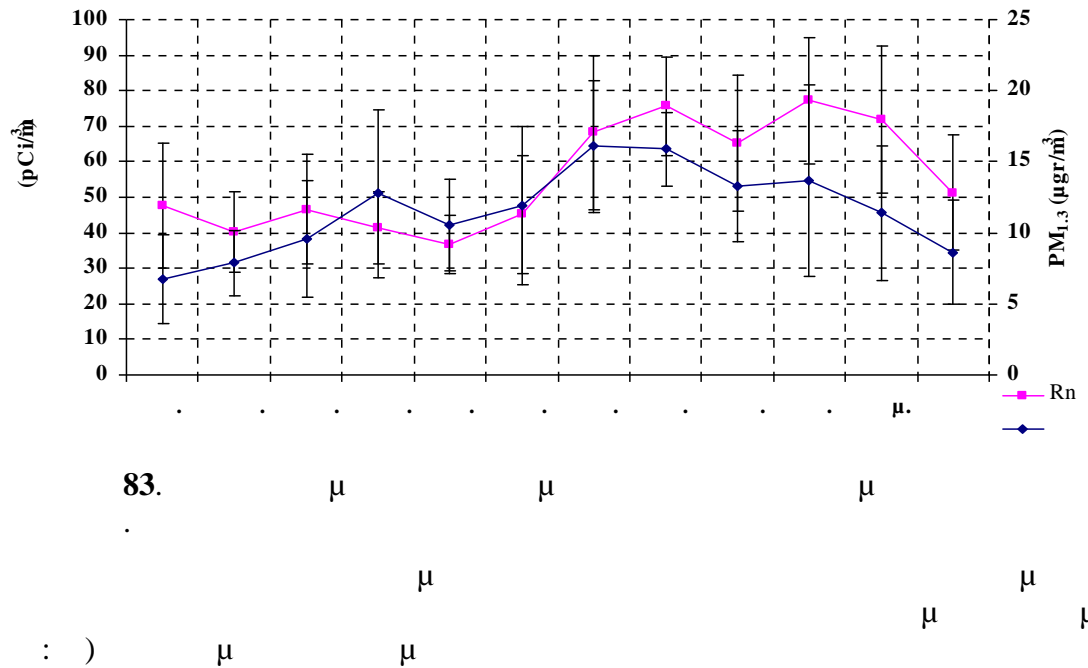
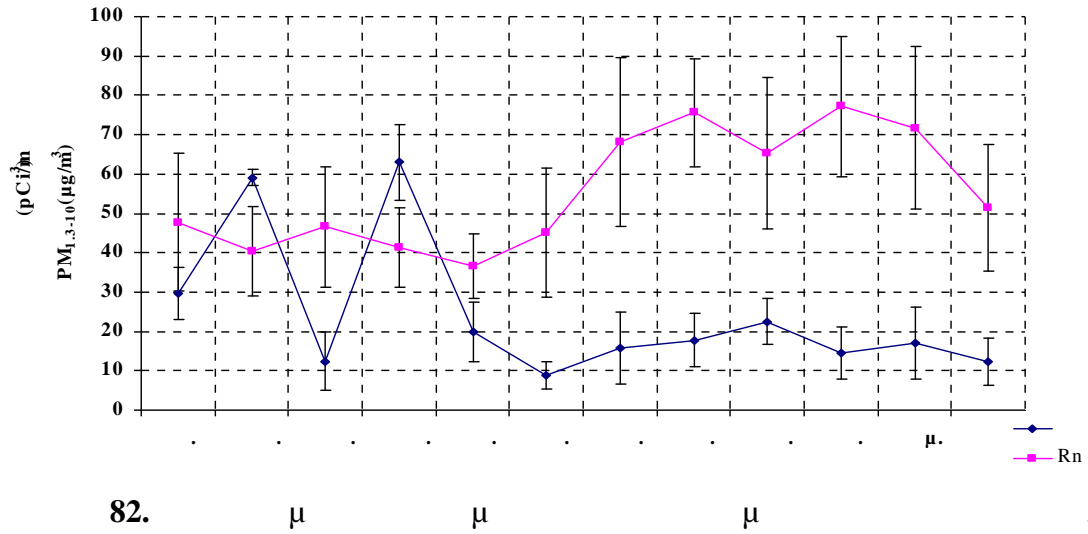
μ

$\mu \quad \mu$

$\mu \quad \mu$

$\mu \quad \mu$

$\mu \quad \mu$



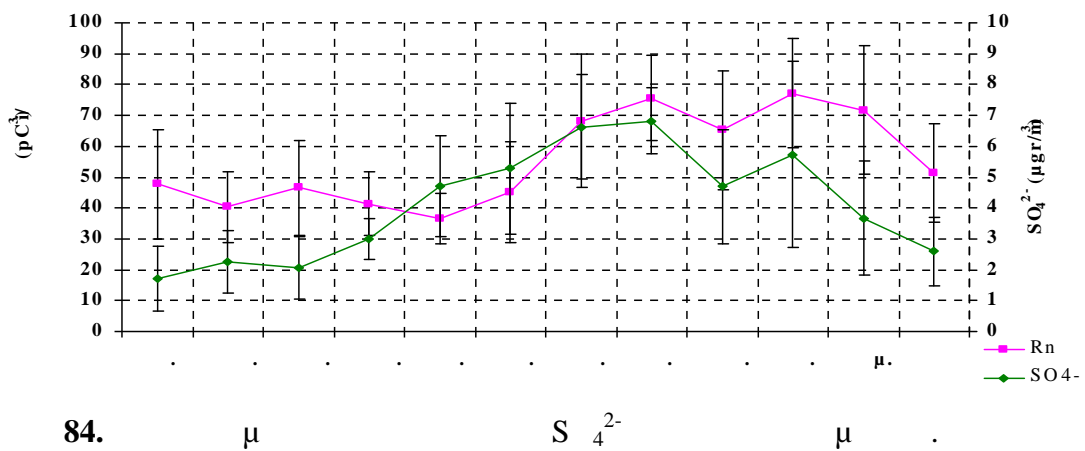
MSA)
 SO_4^{2-} , NH_4^+ , $\text{C}_2\text{O}_4^{2-}$.

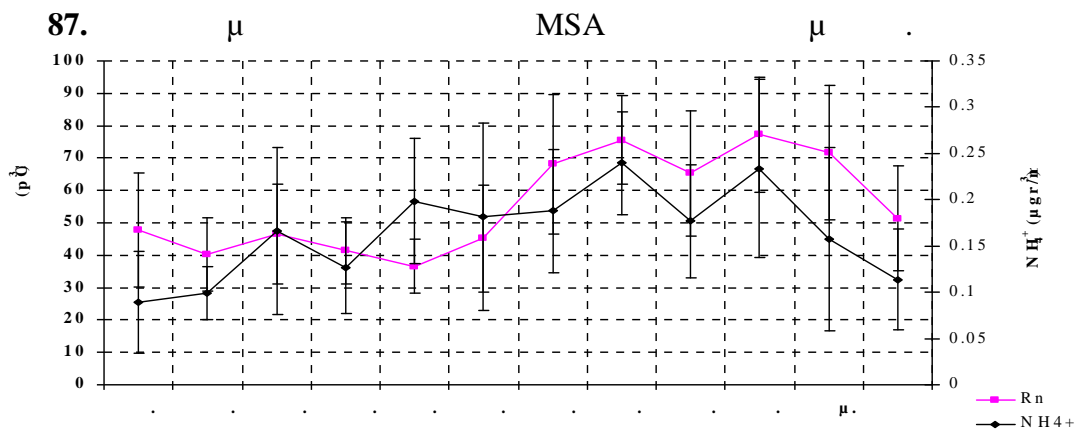
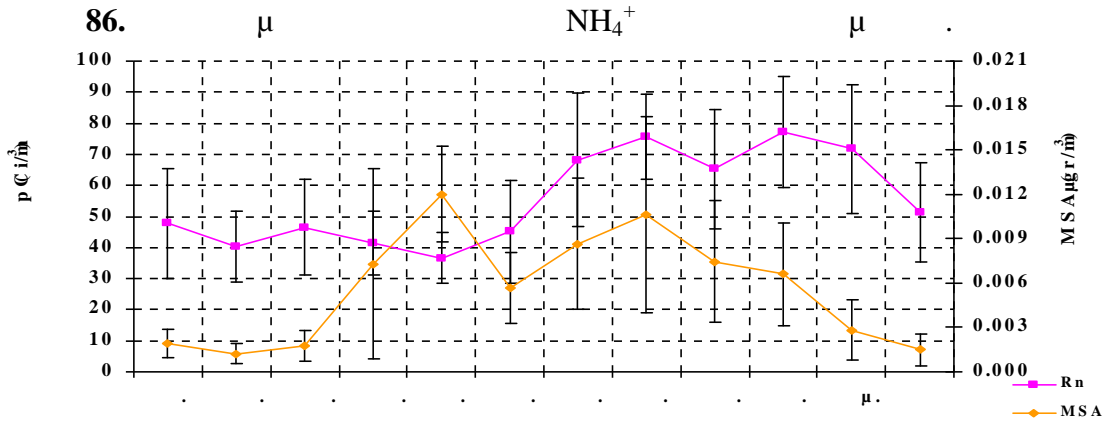
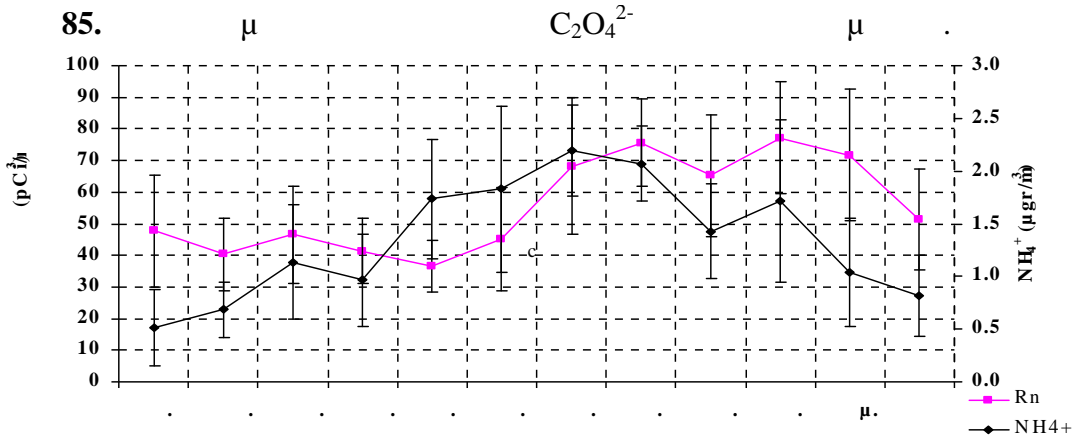
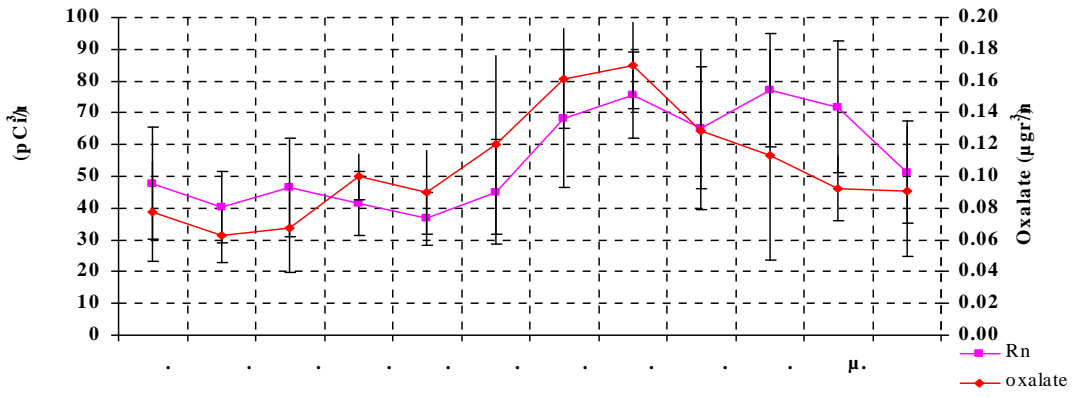
84

88

NH_4^+

O_3^-





6.4. $\mu\mu$ μ μ .

30 μ μ $\mu\mu$

μ μ μ . μ μ μ μ μ 95%.

	(Coarse)		(Fine)		+ (Coarse + Fine)	
	R square (%)	μ .	R square (%)	μ .	R square (%)	μ .
MSA	6,7	95% (+)	16,7	99% (+)	13,5	99% (+)
Cl⁻	7,2	95% (-)	0,8	50% (+)	3,3	90% (-)
NO₃⁻	6,7	95% (+)	0,5	50% (-)	8,3	99% (+)
SO₄²⁻	2,2	80% (+)	49,9	99% (+)	60,9	99% (+)
Oxalate	5,0	95% (+)	38,9	99% (+)	38,9	99% (+)
Na⁺	1,3	65% (-)	0,6	40% (-)	0,6	50% (-)
NH₄⁺	66,2	99% (+)	42,2	99% (+)	49,4	99% (+)
K⁺	2,9	85% (-)	28,2	99% (+)	14,5	99% (+)
Mg²⁺	1,7	73% (-)	0,3	18% (+)	0,6	50% (-)
Ca²⁺	5,9	95% (-)	0,7	38% (-)	5,2	95% (-)
OC	3,3	86% (-)	6,4	95% (+)	0,4	43% (+)
EC	12,8	99% (+)	8,9	99% (+)	10,7	99% (+)
Al	2,7	82% (-)	1,3	70% (+)	2,4	82% (-)
Ca	3,3	87% (-)	1,4	70% (-)	3,0	87% (-)
Ti	1,8	73% (-)	2,1	80% (+)	1,2	65% (-)
V	0,9	53% (+)	27,2	99% (+)	13,8	99% (+)
Cr	9,3	99% (+)	7,6	95% (+)	10,3	99% (+)
Mn	2,3	80% (-)	1,1	65% (-)	2,0	75% (-)
Fe	2,5	82% (-)	2,5	80% (-)	2,3	80% (-)
Ni	6,7	95% (+)	24,1	99% (+)	20,0	99% (+)

30. μ μ μ .

$\mu\mu$ μ μ μ (6,7%), (7,2%),
 $\mu\mu$ μ μ (66,2%) (12,8%).
 μ (16,7%), (49,9%), $\mu\mu$ μ μ (38,9%), $\mu\mu$
(42,2%), (28,2%), μ μ (6,4%),
(8,9%), (27,2%), μ (7,6%),
(24,1%).
 μ 10, $\mu\mu$ μ μ (13,5%), (8,3%)
 μ μ (60,9%), (38,9%), $\mu\mu$ (49,4%), (14,5%),
(5,2%), $\mu\mu$ (10,7%), (13,8%),
 μ (10,3%), (20,0%).

6.5.

(2,5-10,0µm) (<2,5µm)
 Bartlett (10)
 Kaiser-Meyer-Olkin,

µ	
Kaiser-Meyer-Olkin Measure of Sampling Adequacy.	0,730
Bartlett's Test of Approx, Chi-Square Sphericity	1791,027
df	105,000
Sig.	1,2E-304

31. Kaiser-Meyer-Olkin

µ .

µ	
Kaiser-Meyer-Olkin Measure of Sampling Adequacy.	0,659
Bartlett's Test of Approx, Chi-Square Sphericity	688,355
df	136,000
Sig.	1,051E-074

32. Kaiser-Meyer-Olkin

µ .

10	
Kaiser-Meyer-Olkin Measure of Sampling Adequacy.	0,779
Bartlett's Test of Approx, Chi-Square Sphericity	1801,434
df	136,000
Sig.	1,789E-288

33. Kaiser-Meyer-Olkin

10.

Bartlett µ 2
 µ µ
 Kaiser-Meyer-Olkin µ µ
 µ µ
 µ 0,65 µ
 µ µ
 µ µ µ µ
 µ µ µ µ (MSA) µ µ
 µ µ µ µ µ

	Cl ⁻	SO ₄ ⁻²	Na	NH ₄ ⁺	Mg ²⁺	Ca ²⁺	Al	Ca	Mn	C ₃ ⁻²	²²² Rn	NO ₃ ⁻	MSA	Fe	Ti
Cl ⁻	1,000														
SO ₄ ⁻²	0,467	1,000													
Na	0,853	0,313	1,000												
NH ₄ ⁺	-0,390	0,031	-0,263	1,000											
Mg ²⁺	0,830	0,400	0,847	-0,295	1,000										
Ca ²⁺	0,387	0,472	0,207	-0,333	0,519	1,000									
Al	0,465	0,644	0,320	-0,254	0,575	0,830	1,000								
Ca	0,397	0,395	0,278	-0,307	0,566	0,905	0,861	1,000							
Mn	0,450	0,777	0,305	-0,241	0,544	0,849	0,926	0,861	1,000						
C ₃ ⁻²	0,151	0,093	0,138	-0,187	0,398	0,784	0,645	0,825	0,595	1,000					
²²² Rn	-0,245	0,051	-0,103	0,704	-0,130	-0,230	-0,152	-0,184	-0,134	-0,112	1,000				
NO ₃ ⁻	0,352	0,283	0,357	0,210	0,375	0,108	0,075	0,086	0,110	-0,001	0,291	1,000			
MSA	0,182	0,109	0,180	0,184	0,271	0,123	0,063	0,147	0,099	0,050	0,225	0,707	1,000		
Fe	0,439	0,793	0,290	-0,258	0,525	0,832	0,918	0,841	0,997	0,569	-0,157	0,077	0,066	1,000	
Ti	0,387	0,670	0,298	-0,249	0,509	0,808	0,783	0,860	0,937	0,633	-0,150	0,072	0,114	0,936	1,000

34.

μ

μ

.

	MSA	NO ₃ ⁻	SO ₄ ⁻²	Oxalate	NH ₄ ⁺	K ⁺	OC	EC	Ca	V	Mn	Ni	²²² Rn	Na ⁺	Cr	Al	Fe
MSA	1,000																
NO ₃ ⁻	0,264	1,000															
SO ₄ ⁻²	0,559	-0,116	1,000														
Oxalate	0,560	0,078	0,736	1,000													
NH ₄ ⁺	0,519	-0,176	0,888	0,679	1,000												
K ⁺	0,101	-0,205	0,442	0,547	0,490	1,000											
OC	0,105	0,061	0,322	0,398	0,398	0,285	1,000										
EC	0,062	0,036	0,111	0,335	0,105	0,323	0,411	1,000									
Ca	-0,035	0,477	-0,244	-0,216	-0,257	-0,190	0,032	0,116	1,000								
V	0,590	0,061	0,533	0,523	0,502	0,166	0,169	0,136	0,004	1,000							
Mn	0,003	0,436	-0,081	0,019	-0,089	0,070	0,115	0,103	0,828	0,082	1,000						
Ni	0,582	0,081	0,508	0,510	0,471	0,147	0,151	0,143	0,028	0,990	0,082	1,000					
²²² Rn	0,326	-0,140	0,643	0,599	0,565	0,487	0,264	0,293	-0,141	0,452	-0,059	0,425	1,000				
Na ⁺	0,383	0,615	0,210	0,321	0,121	0,012	0,038	-0,040	0,098	0,013	0,236	0,009	-0,080	1,000			
Cr	-0,133	0,475	-0,230	-0,133	-0,288	-0,117	-0,029	0,014	0,828	-0,006	0,926	0,006	-0,169	0,117	1,000		
Al	0,415	0,228	0,234	0,353	0,195	-0,028	0,280	0,285	0,219	0,627	0,162	0,628	0,189	0,018	0,116	1,000	
Fe	0,079	0,609	-0,235	-0,103	-0,242	-0,141	0,050	0,161	0,827	0,111	0,791	0,128	-0,127	0,115	0,790	0,275	1,000

35.

μ

μ

.

	MSA	SO ₄ ²⁻	NH ₄ ⁺	Ca	Mn	Fe	CO ₃ ²⁻	²²² Rn	Na ⁺	Mg ²⁺	Ca ²⁺	Cl ⁻	Cr	Ti	Oxalate	Ni	Al
MSA	1,000																
SO ₄ ²⁻	0,526	1,000															
NH ₄ ⁺	0,520	0,805	1,000														
Ca	-0,069	-0,087	-0,321	1,000													
Mn	-0,065	0,106	-0,252	0,872	1,000												
Fe	-0,098	0,079	-0,291	0,857	0,995	1,000											
CO ₃ ²⁻	-0,008	-0,113	-0,155	0,812	0,586	0,562	1,000										
²²² Rn	0,316	0,629	0,586	-0,177	-0,118	-0,149	-0,099	1,000									
Na ⁺	0,092	-0,056	-0,219	0,261	0,288	0,269	0,150	-0,081	1,000								
Mg ²⁺	0,041	-0,072	-0,277	0,572	0,560	0,546	0,423	-0,093	0,833	1,000							
Ca ²⁺	-0,093	-0,095	-0,336	0,918	0,889	0,880	0,742	-0,220	0,215	0,546	1,000						
Cl ⁻	-0,026	-0,120	-0,329	0,373	0,419	0,405	0,166	-0,181	0,865	0,838	0,396	1,000					
Cr	0,189	0,197	0,097	0,051	0,099	0,107	0,069	0,238	0,209	0,154	0,020	0,112	1,000				
Ti	0,014	0,057	-0,241	0,860	0,919	0,916	0,637	-0,108	0,306	0,527	0,849	0,374	0,174	1,000			
Oxalate	0,564	0,703	0,521	0,260	0,376	0,334	0,234	0,537	0,206	0,289	0,270	0,170	0,358	0,350	1,000		
Ni	0,409	0,438	0,300	0,345	0,405	0,385	0,313	0,393	0,174	0,289	0,309	0,082	0,647	0,464	0,613	1,000	
Al	-0,059	0,036	-0,269	0,878	0,935	0,926	0,646	-0,145	0,314	0,592	0,874	0,456	0,115	0,809	0,377	0,384	1,000

36.

μ

μ

10.(

).

Varimax

Varimax.

Varimax

86,53% , 81,58%, 83,57%

	1	2	3	4
Cl ⁻		0,913		
SO ₄ ²⁻				0,795
Na		0,909		
NH ₄ ⁺			0,678	
Mg ²⁺		0,823		
Ca ²⁺	0,932			
Al	0,862			
Ca	0,953			
Mn	0,883			
CO ₃ ²⁻	0,859			
²²² Rn			0,729	
NO ₃ ⁻			0,761	
MSA			0,754	
Fe	0,868			
Ti	0,872			
μ	6,07	3,25	2,18	1,48
% μ	40,48	21,64	14,54	9,88
μ	40,48	62,11	76,65	86,53

37. μ Varimax

	1	2	3	4	5
MSA		0,343	0,617	0,488	
NO ₃ ⁻	0,463			0,732	
SO ₄ ²⁻		0,827	0,340		
Oxalate (C ₂ O ₄ ²⁻)		0,722	0,335		
NH ₄ ⁺		0,821			
K ⁺		0,767			
OC					0,720
EC					0,850
Ca	0,905				
V		0,343	0,895		
Mn	0,956				
Ni		0,311	0,901		
²²² Rn		0,715			
Na ⁺				0,925	
Cr			0,792		
Al	0,874				
Fe	0,953				
μ	3,75	3,57	3,10	1,85	1,60
% μ	22,07	21,02	18,23	10,86	9,39
μ	22,07	43,09	61,32	72,18	81,58
			,		
			.		

38.

μ Varimax

μ

24

(14,50%) 4,20% 1,5%

. Gerasopoulos et.al.,2006, 2005, D. Desideri at al., 2006, L.Sesana et al.,1998).

2002-2006

31,5%

60 pCi/m³.

2002). μ μ MSA μ (,
 $C_2O_4^{2-}$, $C_2O_4^{2-}$, SO_4^{2-} μ
 $C_2O_4^{2-}$, SO_4^{2-} .

7.2.

- μ μ μ μ μ μ
 μ μ μ μ μ μ
 :
- i. μ 5 μ μ
 μ μ μ μ μ , μ μ
 μ μ μ μ μ . μ μ
- ii. μ
 (Positive Matrix Factorization)
 (μ)
 μ μ μ μ (Potential Source
 Contribution Function) μ
- iii. μ μ μ μ μ μ
 μ μ μ μ μ μ
 μ μ μ μ μ μ

- A. El-Hussein, A. Mohammed and A. A. Ahmed A, Study on radon and radon progeny in surface air of El Minia, Egypt, 1998.
- Alexander V. Polissar and Philip K. Hopke, Richard L. Poirot Atmospheric Aerosol over Vermont: Chemical Composition and Sources, 2001.
- Arrigo A. Cigna, Radon in Caves, International Journal of Speleology, 2005.
- Barbara Hennemuth and Andrea Lammert , Determination of the atmospheric boundary layer height from radiosonde and lidar backscatter, 2006
- Boutsikas M.V., μ , μ μ « , $\mu\mu$ » μ μ . & μ , μ , μ , 2004.
- C. Dueñas, M. Pèrez, M.C. Fernández & j. Carretero, Radon Concentrations in Surface air and vertical atmospheric stability of the lower atmosphere, 1994.
- C. Richard Cothern and Janes E. Smith, Jr., Environmental Radon, Plenum Press New York, 1987.
- Cally Oldershaw, The Geological Society of London, The earth is in our hands, 2001.
- Charles R.Hosler, Natural Radioactivity (Radon-222) and Air pollution Measurements in Wasington, D.C. 1966
- C. Matti, A. Pauling, M. Kuttel, H. Wanner; Winter precipitation trends for two selected European regions, over the last 500 years and their possible dynamical background, 2008.
- C. Papastefanou et al., Radon measurements along active faults in the Langadas Basin, northern Greece, 2001.
- D. Desideri, C. Roselli, M. A. Meli, L. Feduzi, Comparison between the diurnal trends of ozone and radon gas concentrations measured at ground in the semi-rural site of Central Italy, 2006.
- D. Morelli, S. Di Martino, G. Immè, S. La Delfa, S. Lo Nigro, G. Patanè Evidence of soil radon as tracer of magma uprising in Mt. Etna, 2006.
- Davud K. Lasch, On Radon Virginia Minerals, 1988
- E. Gerasopoulos, G. Kouvarakis, M. Vrekoussis, M. Kanakidou, and N. Mihalopoulos, Ozone variability in the marine boundary layer of the eastern Mediterranean based on 7-year observations, 2005
- E. Koulouri, S. Saarikoski, C. Theodosi, Z. Markaki, E. Gerasopoulos, G. Kouvarakis, T. Mäkelä, R. Hillamo N. Mihalopoulos, Chemical composition and sources of fine and coarse aerosol particles in the Eastern Mediterranean, 2008.
- E. M. Fischer and S.I. Seneviratne, P.L. Vidale, D. Lüthi and C. Schär, Soil Moisture–Atmosphere Interactions during the 2003 European Summer Heat Wave, 2007.
- Evangelos Gerasopoulos, Giorgos Kouvarakis, Mihalis Vrekoussis, Christos Donoussis, Nikolaos Mihalopoulos, Maria Kanakidou, Photochemical ozone production in the Eastern Mediterranean, 2005.

- F. Conen and L. B. Robertson, Latitudinal distribution of radon-222 flux from continents, 2001.
- Fernando P. Carvalho, Origins and concentrations of ^{222}Rn , ^{210}Pb , ^{210}Bi and ^{210}Po in the surface air at Lisbon Portugal, at the Atlantic edge of the European continental landmass, 1995.
- Frank Dentener, Johann Feichter and Ad Jeuken, Simulation of the transport of Rn^{222} using on-line and off-line global models at different horizontal resolutions: a detailed comparison with measurements, 1998.
- G. J. van Oldenborgh, How unusual was autumn 2006 in Europe?, 2007.
- H. Bardouki et al.: Gaseous (DMS , MSA , SO_2 , H_2SO_4 and DMSO) and particulate (sulfate and methanesulfonate) sulfur species over the northeastern coast of Crete, 2003.
- H. Wollenberg, S. Flexser, G. Brimhall, and C. Lewis, Radon Sources and Emanation in Granitic Soil and Saproliite, 1993.
- H. Zafri, The Evolution, Transportation and Variation in Time of Rn^{222} Within Rocks in a Desert Region, 2008.
- Hajime Akimoto, Prabir Patra, Kentaro Ishijima, Masayuki Takigawa, Shamil Maksyutov, Takashi Maki, Atmospheric Composition Change and its Climate Effect Studied by Chemical Transport Models, 2006.
- J C H Miles and R A Algar, Variations in radon-222 concentrations, 1988.
- J. Kysely and R. Huth, Relationships of surface air temperature anomalies over Europe to persistence of atmospheric circulation patterns conducive to heat waves, 2008.
- J. Sciare, H. Bardouki, C. Moulin, and N. Mihalopoulos, Aerosol sources and their contribution to the chemical composition of aerosols in the Eastern Mediterranean Sea during summertime, 2003.
- J. Sciare, K. Oikonomou¹, O. Favez¹, E. Liakakou, Z. Markaki, H. Cachier, and N. Mihalopoulos, Long-term measurements of carbonaceous aerosols in the Eastern Mediterranean: evidence of long-range transport of biomass burning
- J.-F. Vinuesa and S. Galmarini, Characterization of the ^{222}Rn family turbulent transport in the convective atmospheric boundary layer, 2007
- J.-F. Vinuesa, S. Basu, and S. Galmarin, The diurnal evolution of ^{222}Rn and its progeny in the atmospheric boundary layer during the Wangara experiment, 2006
- Jiyoung Kim, Soon-Chang Yoon, Anne Jefferson, Wlodek Zahorowski, Chang-Hee Kang, Air mass characterization and source region analysis for the Gosan super-site, Korea, during the ACE-Asia 2001 field campaign, 2005.
- John E. Pearson and Harry Moses, Atmospheric Variation with Height and time. Argonne national Laboratory, 1965.
- K. Wattanikorn, M. Kanaree and S. Wiboolsake, Soil gas Radon as an earthquake precursor: some considerations on data improvement, 1998.

- K. Zhang, H. Wan, M. Zhang, and B. Wang, Evaluation of the atmospheric transport in a GCM using radon measurements: sensitivity to cumulus convection parameterization, 2008.
- Karl K. Turekian, Y. Nozaki, and Larry K. Benniger, Geochemistry of atmospheric radon and products, 1977.
- Kaushik Majumdar, A study of fluctuation in radon concentration behaviour as an earthquake precursor, 2004
- L. Sesana, L. Barbieri, U. Facchini and G. Marazzan, ^{222}Rn as a tracer of atmospheric Motions: A study in Milan, 1998.
- L. Zhang et al., Atmospheric radon levels in Beijing, China, 2004.
- Lynette B. Robertson, David S. Stevenson and Franz Conen, Test of a northwards-decreasing ^{222}Rn source term by comparison of modelled and observed atmospheric ^{222}Rn concentrations, 2004.
- Mohan L. Gupta, Anne R. Douglass, S. Randolph Kawa, Steven Pausan, Use of radon for evaluation of atmospheric transport models: sensitivity to emissions, 2004.
- Nikolaos Mihalopoulos, Long – range transport of pollutants above the eastern Mediterranean: Implications for air quality and regional climate, 2007.
- P. Martin, S. Tims, B. Ryan, A. Bollhöfer, A radon and meteorological measurement network for the Alligator Rivers Region, Australia, 2003.
- Piero Di Carlo, Giovanni Pitari, Natalia De Luca, Domenico Battisti, Observations of surface radon in Central Italy, 2008
- R. Randall Schumann and Linda C.S. Gundersen, Geologic and climatic controls on the radon emanation coefficient, 1996.
- S. E. Gryning, the height of the atmospheric boundary layer during unstable conditions, 2005.
- S. Whittlestone and E. Robinson and S. Ryan, Radon at the Mauna Loa Observatory transport from distant continents, 1991.
- S. Whittlestone, Radon measurements as an aid to the interpretation of atmospheric monitoring, 1985.
- Stanley S. Johnson, Natural radiation, Virginia minerals, 1991.
- Tao Wang, Wlodek Zahorowski, Receptor modelling using Positive Matrix Factorisation, back trajectories and Radon-222, 2007
- Ta-Yung Li, Diurnal variations of radon and meteorological variables near the ground, 1974.
- 2002.
- W. Zahorowski, S.D. Chambers, A. Henderson-Sellers Ground based radon-222 observations and their application to atmospheric studies, 2003.
- Wen – Jie Zhang et.al. Characteristics and seasonal variation of $\text{PM}_{2.5}$, PM_{10} TSP aerosol in Beijing., 2006.
- William W. Nazaroff, Radon Transport from Soil to Air, 1992.

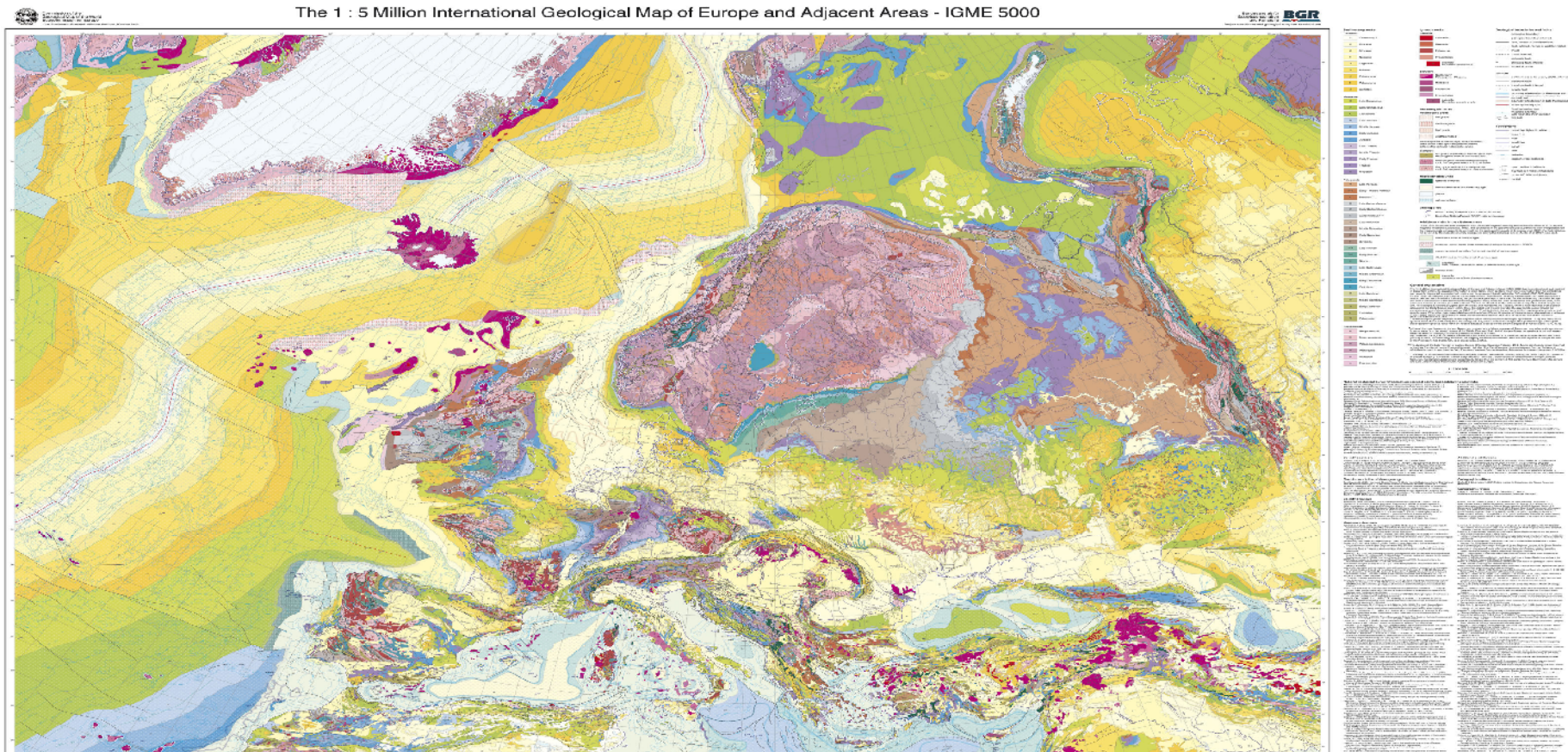
Wlodek Zahorowski, Scott Chambers, Tao wang, Chang-Hee Kang, Itsushi Uno, Steven Poon, Sung-Nam Oh, Sylvester Werczynski, Jiyoung Kim and Ann Henderson – Sellers, Radon in boundary layer and free tropospheric continental outflow events ai three ACE- Asia sites, 2004.

Yves j. Balkanski and Daniel J. Jacob, Transport of continental air to the subantarctic Indian Ocean, 1989.

μ , μ μ
μ , 2007.
K. , μ μ ,
μ μ SPSS.
μ , . 2008
μ , , 2005.

μ :

.



89. μ . μ 1:5 $\mu\mu$. (CCGM CGMW Commission of the Geological map of the World, Sub commission for Europe).

Sedimentary rocks

Cenozoic

Q	Quaternary*
N2	Pliocene
N1	Miocene
N	Neogene
E3	Oligocene
E2	Eocene
E1	Palaeocene
E	Palaeogene
CZ	Cenozoic

Mesozoic

K2	Late Cretaceous
K1	Early Cretaceous
K	Cretaceous
J3	Late Jurassic
J2	Middle Jurassic
J1	Early Jurassic
J	Jurassic
T3	Late Triassic
T2	Middle Triassic
T1	Early Triassic
T	Triassic
M2	Mesozoic

Palaeozoic

P3-3	Middle - Late Permian
P1	Early Permian
P	Permian
C2	Late Carboniferous
C1	Early Carboniferous
C	Carboniferous
D3	Late Devonian
D2	Middle Devonian
D1	Early Devonian
D	Devonian
S3-1	Late Silurian
S1-2	Early Silurian
S	Silurian
O3	Late Ordovician
O2	Middle Ordovician
O1	Early Ordovician
O	Ordovician
€3	Late Cambrian
€2	Middle Cambrian
€1	Early Cambrian
€	Cambrian
P2	Palaeozoic

Precambrian

NP	Proterozoic III
MP	Proterozoic II
PP	Proterozoic I
PR	Proterozoic
AR	Archaean
PC	Precambrian

Igneous rocks

Intrusive

	Cenozoic
	Mesozoic
	Palaeozoic
	Precambrian
N1	example: Miocene intrusive rock

extrusive

	Cenozoic
	Mesozoic
	Palaeozoic
	Precambrian
C	example: Cambrian extrusive rock

Metamorphic rocks

metamorphic grade

	low grade
	medium grade
	high grade
	undifferentiated

Depending on their origin, metamorphic rocks are displayed as a combination of the colour of the protolith and the pattern of its particular metamorphic grade.

	metamorphic rock, protolith undivided
--	---------------------------------------

Examples:

	low grade sedimentary metamorphic rock, first orogenic event in the Palaeozoic
	medium grade extrusive metamorphic rock, first orogenic event in Precambrian
	high grade metamorphic rock, protolith undivided

Miscellaneous units

	ophiolite complex
	glacier
	aeolian sediments of Quaternary age
	salt pan or lake

Drilling sites

602	Ocean Drilling Program (ODP), site and number
134	Deep Sea Drilling Project (DSDP), site and number

Additional units in the off-shore areas

The geological boundaries were derived from the magnetic sea-floor spreading anomalies (Cande et al., 1989) and transferred into standard geological time (geochronological) subdivisions using the geomagnetic polarity timescale of Cande & Kent (1995). For high latitudes, not covered by the map of magnetic anomalies from Cande et al. (1989), ocean crustal ages were estimated from the digital age grid of Müller et al. (1997). The resulting isochrons were controlled and adjusted by comparison with the magnetic anomaly map of the Arctic and North Atlantic oceans of Verhoef et al. (1996).

	continental crust of various ages
	ocean-continent transition (exhumed mantle) of various ages
	rifted thinned continental crust of various ages
MZ	example: rifted thinned continental crust of Mesozoic/unknown age
	oceanic crust
Ka	example: oceanic crust of Late Cretaceous age
	fold belt

General explanation

All geological units (sedimentary, igneous and metamorphic) on the map are identified by a colour code and an abbreviation indicating the geochronological age of the rock. For sedimentary rocks the age and colours subdivisions of the International Stratigraphic Chart (Flemens et al. 2000/2004) were used: transitional and general units like Permo-Triassic, Mesozoic or undifferentiated Triassic are shown in the colour of the respective oldest unit, e.g. Mesozoic is marked with the colour of Triassic which itself receives the colour of Early Triassic (dark violet). Thus, the oldest unit characterises the whole rock unit. Abbreviations within the polygon on the map may give the exact age indication, such as MZ, T, T1, P-1. Geological units of the same age but of different lithology are treated as separate geological units in the map-related database. On the map they will share the same colour, but are distinguished by a geological boundary when adjacent to each other. The metamorphic grade follows the classification of Winkler (1976) and Frey et al. (2002). The classification of igneous rocks is based on Streckeisen (1975, 1978).

*Although the map focuses on the pre-Quaternary on- and off-shore geology, all Quaternary extrusive rocks are shown. In some areas (e.g. the desert regions of the Middle East and North Africa) the pre-Quaternary geology is not well known. Here the extent of the cover of Quaternary aeolian sediments is shown.

Geological and faults boundaries general

—	geological boundary
- - - -	geological boundary, inferred
— — —	fault, normal or undifferentiated
- - - - -	fault, inferred, normal or undifferentiated
· · · · ·	thrust
- · · · · -	thrust, inferred
— — —	strike/slip fault
- - - - -	strike/slip fault, inferred
· · · · ·	impact structure

off-shore

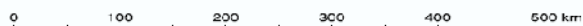
	ocean-continent boundary
— — —	transform fault
- - - - -	transform fault, inferred
— — —	gravity fault
- - - - -	boundary of extension of Messinian salt, inferred
- - - - -	boundary of extension of Triassic to Jurassic salt, inferred
- - - - -	boundary of extension of Triassic to Jurassic salt, inferred
— — —	active spreading axis
- - - - -	fossil spreading axis

Topography

—	coast, highlighted in white
— — —	large river
— — —	river
— — —	small river
· · · · ·	canal
— — —	lake
— — —	isobaths

○ Lyon	over 1 million inhabitants
○ Kidal	100 000 to 1 million inhabitants
○ Vaasa	under 100 000 inhabitants
MADRID	capital

1 : 5 000 000



μ III:

Einstein, $E = m \cdot c^2$.

« »

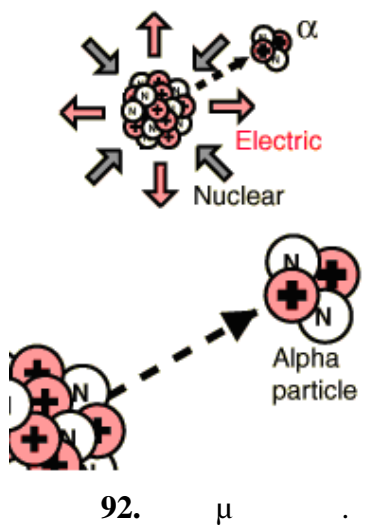
(μ)

()

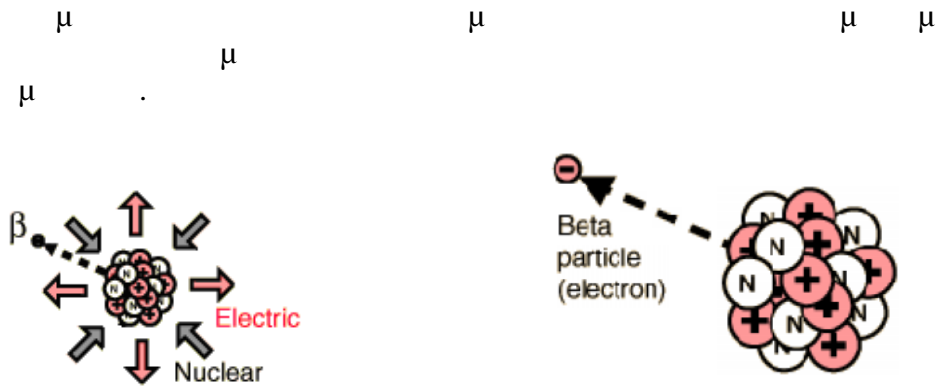
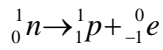
()

μ μ μ

1. (μ): μ 7000 μ



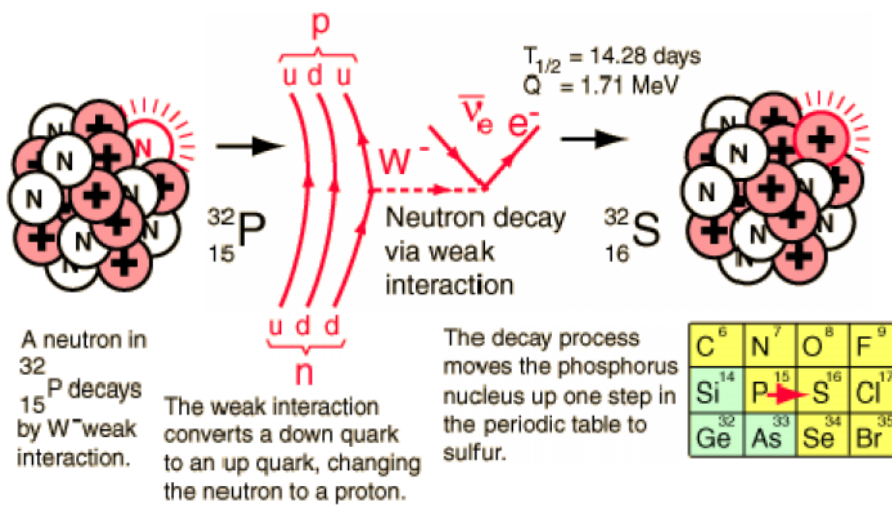
2. (μ): μ μ μ



93.

(weak interaction)

Feynman.



94. Feynman.

3.

μ $\mu\mu$ (μ): μ μ μ
 10^{-12} m, μ μ μ
 μ μ μ
 μ μ μ μ
 μ μ μ μ μ μ μ μ μ μ

